# The lysosomal membrane protein LAMP2A promotes autophagic flux and prevents SNCA-induced Parkinson disease-like symptoms in the Drosophila brain

Abdul-Raouf Issa, Jun Sun, Céline Petitgas, Ana Mesquita, Amina Dulac, Marion Robin, Bertrand Mollereau, Andreas Jenny, Baya Chérif-Zahar, Serge Birman

# The lysosomal membrane protein LAMP2A promotes autophagic flux and prevents SNCA-induced Parkinson disease-like symptoms in the *Drosophila* brain

Abdul-Raouf Issa[1], Jun Sun[1], Céline Petitgas[1], Ana Mesquita[2], Amina Dulac[1], Marion Robin[3], Bertrand Mollereau[3], Andreas Jenny[2], Baya Chérif-Zahar[1], and Serge Birman[1,*]

[1]Genes Circuits Rhythms and Neuropathology, Brain Plasticity Unit, CNRS, ESPCI Paris, PSL Research University, 10 rue Vauquelin, F-75005 Paris, France

[2]Albert Einstein College of Medicine, Jack and Pearl Resnick Campus, 1300 Morris Park Avenue, Chanin Building, Room 503, Bronx, NY 10461, United States

[3]Université de Lyon, ENSL, UCBL, CNRS, LBMC, UMS 3444 Biosciences Lyon Gerland, 46 Allée d'Italie, F-69007, Lyon, France

*Author for correspondence: serge.birman@espci.fr

Running title: Neuroprotection by LAMP2A in *Drosophila*

## Key words

autophagy-lysosome pathway; *Drosophila melanogaster;* endosomal microautophagy; macroautophagy; neuroprotection; oxidative stress; Parkinson disease model; synuclein alpha (SNCA)

## Abstract

The autophagy-lysosome pathway plays a fundamental role in the clearance of aggregated proteins and protection against cellular stress and neurodegenerative conditions. Alterations in autophagy processes, including macroautophagy and chaperone-mediated autophagy (CMA), have been described in Parkinson disease (PD). CMA is a selective autophagic process that depends on LAMP2A (Lysosomal associated membrane protein 2A), a mammal and bird-specific membrane glycoprotein that translocates cytosolic proteins containing a KFERQ-like peptide motif across the lysosomal membrane. *Drosophila* reportedly lack CMA and use endosomal microautophagy (eMI) as an alternative selective autophagic process. Here we report that neuronal expression of human LAMP2A protected *Drosophila* against starvation and oxidative stress, and delayed locomotor decline in aging flies without extending their lifespan. LAMP2A also prevented the progressive locomotor and oxidative defects induced by neuronal expression of PD-associated human SNCA (synuclein alpha) with alanine-to-proline mutation at position 30 ($SNCA^{A30P}$). Using KFERQ-tagged fluorescent biosensors, we observed that LAMP2A expression stimulated selective autophagy in the adult brain and not in the larval fat body, but did not increase this process under starvation conditions. Noteworthy, we found that neurally expressed LAMP2A markedly upregulated levels of *Drosophila* Atg5, a key macroautophagy initiation protein, and of the Atg5-containing complex, and that it increased the density of Atg8a/LC3-positive puncta, which reflects the formation of autophagosomes. Furthermore, LAMP2A efficiently prevented accumulation of the autophagy defect marker Ref(2)P/p62 in the adult brain under acute oxidative stress. These results indicate that LAMP2A can promote

autophagosome formation and potentiate autophagic flux in the *Drosophila* brain, leading to enhanced stress resistance and neuroprotection.

## Abbreviations

Act5C: actin 5C; a.E.: after eclosion; Atg5: autophagy-related 5; Atg8a/LC3: autophagy-related 8a; CMA: chaperone-mediated autophagy; DHE: dihydroethidium; elav: embryonic lethal abnormal vision; eMI: endosomal microautophagy; ESCRT: endosomal sorting complexes required for transport; GABARAP: GABA typeA receptor-associated protein; Hsc70-4: heat shock protein cognate 4; HSPA8/Hsc70: heat shock protein family A (Hsp70) member 8; LAMP2: lysosomal associated membrane protein 2; MDA: malondialdehyde; PA-mCherry: photoactivable mCherry; PBS: phosphate-buffered saline; PCR: polymerase chain reaction; PD: Parkinson disease; Ref(2)P/p62: refractory to sigma P; ROS: reactive oxygen species; RpL32/rp49: ribosomal protein L32; RT-PCR: reverse transcription polymerase chain reaction; SING: startle-induced negative geotaxis; SNCA/α-synuclein: synuclein alpha; SQSTM1/p62: sequestosome 1; TBS: Tris-buffered saline; UAS: upstream activating sequence.

## Introduction

Autophagy is an essential cellular process conserved in all eukaryotic systems that degrades or recycles cellular components through delivery to lysosomes and plays essential function in development, cell physiology and protection against various stresses and diseases [1-4]. Three main autophagic pathways are described: macroautophagy, microautophagy and chaperone-

mediated autophagy (CMA). Macroautophagy involves the formation of a phagophore that sequesters parts of the cytoplasm, including protein aggregates or organelles such as damaged mitochondria (mitophagy); upon completion, the phagophore matures into a double-membrane autophagic vesicle (autophagosome). The autophagosomes then fuse with lysosomes leading to degradation of the vesicle content [4-6]. Microautophagy in contrast only implicates lysosomes or late endosomes that directly entrap cytoplasmic materials or proteins by membrane invagination [7-9].

Approximately 30% of cytosolic proteins contain a KFERQ-like pentapeptide motif [10] recognized by the chaperone HSPA8/Hsc70 (heat shock protein family A [Hsp70] member 8) [11,12]. These proteins are selectively degraded either by endosomal microautophagy (eMI), which involves engulfment by late endosomes [8,13,14], or, alternatively, by CMA, in which the substrate proteins are unfolded and translocated one by one through the lysosomal membrane [15-17]. CMA depends on the LAMP2A (Lysosomal associated membrane protein 2A) receptor, a membrane glycoprotein involved in protein translocation from the cytosol to the lysosomal lumen [18]. Structurally, LAMP2A consists of a heavily glycosylated large N-terminal lumenal domain, a single transmembrane spanning region and a short (12 amino acids) C-terminal tail exposed in the cytosol [19,20]. Alternative splicing of the human *LAMP2* gene produces 3 protein isoforms (LAMP2A, LAMP2B and LAMP2C) that each carries out specific roles in autophagy [19,21], but only LAMP2A can function in CMA [22].

CMA alterations have been observed in several neuropathologies, including Parkinson disease (PD), Alzheimer disease and Huntington disease, in which neurodegenerative symptoms are associated with the accumulation of aberrant protein oligomers or aggregates [15,16,23-25].

Pathogenic mutations in 2 PD-associated genes, *SNCA* (*synuclein alpha*) and *LRRK2* (*leucine rich repeat kinase 2*), have been reported to disrupt CMA-mediated cytosolic protein degradation [26,27]. Enhancing CMA through LAMP2A overexpression in the rat substantia nigra counteracts SNCA pathogenicity, leading to lower SNCA levels and decreased dopaminergic neuron degeneration [28]. This indicates that CMA is a potential target to prevent or treat PD and other neuropathologies.

*Drosophila* is a widely used model to study the mechanisms and regulations of autophagy *in vivo* [29-32]. In this organism, macroautophagy has prominent developmental functions [33] and plays a protective role against starvation and oxidative stress [34,35], whereas eMI is required for protein turnover at synapses [13] and to be induced by prolonged starvation [14]. The LAMP2A protein contains in its C-terminal tail a specific peptide motif required for CMA that is known to be present only in mammals and birds. This suggests that CMA does not occur in *Drosophila* [13,14].

Here, in order to learn more about LAMP2A-mediated neuroprotective mechanisms, we studied whether this protein can act as a stress-protectant in the fly. We show that the pan-neuronal expression of human LAMP2A is sufficient to significantly enhance *Drosophila* resistance to various stresses, and to protect against mutant SNCA pathogenicity and prolong locomotor ability in aging flies. By using eMI fluorescent sensors and antibodies against autophagy-related proteins, we found that LAMP2A expression promoted both selective autophagy and autophagosome formation in the fly brain. LAMP2A also prevented Ref(2)P/SQSTM1/p62 (Refractory to sigma P) accumulation under oxidative stress, indicating that the neural expression of this lysosomal protein can stimulate autophagic flux in *Drosophila*.

## Results

### *Neuronal LAMP2A expression protects flies from starvation and oxidative stress*

To study the function of the human LAMP2A receptor in *Drosophila*, we generated *UAS-LAMP2A* strains. Pan-neuronal (*elav>LAMP2A*) expression yielded viable fly progeny that developed normally to adults and did not have apparent behavioral defects. Reverse transcription polymerase chain reaction (RT-PCR) analysis performed on adult head RNA extracts from these flies, as well as whole-mount brain immunostaining with a specific antibody, confirmed the transgenic expression and stability of human LAMP2A in the fly (Fig. S1A and B). We then examined the effects of the neural expression of this protein on *Drosophila* resistance to nutrient deprivation, a typical inducer of autophagy. A significant protection against prolonged (>24 h) starvation was observed when LAMP2A was ectopically expressed in all *Drosophila* neurons (Fig. 1A, see statistical data in Table S3). While the median survival was ~48 h for control starved flies, it rose to ~72 h for *elav>LAMP2A* flies in the same conditions. This higher resistance suggests that human LAMP2A expression enhances autophagy in *Drosophila*.

Oxidative stress promotes protein damage and aggregation that can be mitigated by increased autophagy [15,35,36]. ROS produced mainly from mitochondrial source under starvation or other stressful conditions can directly induce autophagy by a mechanism that is not fully understood [37]. Increased *LAMP2A* transcription and CMA activation were previously demonstrated in rats under paraquat-mediated oxidative stress [38]. Here we find that flies with pan-neuronal LAMP2A expression showed much higher tolerance to paraquat compared to the driver and UAS controls: around 50% of LAMP2A flies were still alive after 72 h of paraquat

exposure, at a time when all control flies were dead (Fig. 1B). Therefore, LAMP2A potently protects *Drosophila* neurons against acute oxidative stress.

***LAMP2A delays locomotor senescence but does not prolong lifespan***

Previous studies showed that restoring CMA by increasing LAMP2A levels could protect from age-related liver function decline in mice [39]. Here we monitored startle-induced negative geotaxis (SING), a frequently used behavioral paradigm to test for locomotor ability in *Drosophila*. SING progressively declines with age or in various mutant neuropathological conditions [40-45]. We observed that flies expressing human LAMP2A in neurons had a better preservation of climbing performance with age compared to controls, which was prominent after 6 weeks of adult life (Fig. 1C). In contrast and interestingly, neuronal LAMP2A expression did not extend *Drosophila* longevity, indicating that it increased fly healthspan rather than lifespan (Fig. 1D).

***LAMP2A coexpression reduces neuronal SNCA accumulation and prevents SNCA$^{A30P}$-induced locomotor defects***

Accumulation of the chaperone protein SNCA plays a central role in PD pathogenesis [46]. This accumulation is normally mitigated by proteasomal degradation and lysosomal clearance, involving in particular CMA activation through LAMP2A and HSPA8 induction [47,48]. SNCA mutations promote protein aggregation and disrupt CMA [26], and this probably contributes to neuronal loss and subsequent motor symptoms in PD. Furthermore, regional variations in CMA activity and LAMP2A expression appear to correlate with differential vulnerability of brain

regions to protein aggregation [49]. Both *LAMP2A* and *HSPA8* mRNAs and proteins are reduced in the substantia nigra pars compacta of PD patients, leading to lower CMA activity and increased SNCA level [50,51].

In *Drosophila*, the expression of human mutant SNCA (alanine-to-proline at position 30, $SNCA^{A30P}$) in neurons causes precocious locomotor impairments in aging flies [40,42,52-54]. Remarkably, we observed that the SING defects induced by neuronal accumulation of $SNCA^{A30P}$ (*elav>*$SNCA^{A30P}$ flies) were fully prevented when LAMP2A was coexpressed (*elav>LAMP2A*, $SNCA^{A30P}$) (Fig. 2A). We also observed a reduced accumulation of $SNCA^{A30P}$ protein in 30-day-old flies when human LAMP2A was coexpressed with the pathogenic protein in all neurons (Fig. 2B). Neither $SNCA^{A30P}$ nor *LAMP2A* mRNA levels were decreased when these transgenes were coexpressed compared to each protein alone (Fig. S2A), indicating that the reduced accumulation of $SNCA^{A30P}$ protein was not related to the presence of 2 UAS transgenes in the genome. The lower $SNCA^{A30P}$ accumulation in *elav>LAMP2A*, $SNCA^{A30P}$ flies compared to *elav>*$SNCA^{A30P}$ is therefore likely to result from a faster degradation of the pathogenic mutant protein. This further indicates that human LAMP2A can activate autophagic clearance in flies. Taken together, these observations are reminiscent of the neuroprotective effect of LAMP2A overexpression in the rat substantia nigra, which prevents dopaminergic neurodegeneration induced by human SNCA and reduces SNCA levels in this PD model as well [28].

***LAMP2A prevents SNCA-induced ROS accumulation and oxidative defects***

Previous reports in *Drosophila* and mouse suggest that the neurotoxicity of SNCA could be partly caused by an increase in oxidative stress associated with the abnormal accumulation of

this protein [52,55-58]. This prompted us to analyze the levels of reactive oxygen species (ROS) in whole-mount *Drosophila* brains using dihydroethidium (DHE) dye fluorescence. Flies coexpressing $SNCA^{A30P}$ together with LAMP2A in all neurons showed significantly decreased ROS abundance compared to flies expressing $SNCA^{A30P}$ alone, both at 2 and 30 days after eclosion (a.E.) (Fig. 2C and Fig. S2B). We also determined the brain level of malondialdehyde (MDA), a compound used to assess the level of lipid peroxidation, as a test for oxidative stress-induced damage [59,60]. While the MDA amount in brain was found to be elevated in the presence of $SNCA^{A30P}$, particularly in 30-day old flies, coexpression of LAMP2A in neurons fully restored brain MDA to normal levels (Fig. 2D). This shows that LAMP2A can counteract the noxious pro-oxidant effect of mutant $SNCA^{A30P}$ in the *Drosophila* brain.

***LAMP2A increases KFERQ motif-selective autophagy in the adult brain of fed flies but not in the larval fat body***

In mammals, LAMP2A is a limiting step for CMA and changes in its levels modulate CMA activity [61]. All conditions known to activate CMA, including prominently starvation, up-regulate LAMP2A level at the lysosomal membrane [38,61,62]. Protection against starvation, oxidative stress and $SNCA^{A30P}$ conferred by LAMP2A expression in *Drosophila* suggests that this protein may be able to stimulate a KFERQ motif-selective autophagy process in this organism. A fluorescent biosensor containing a KFERQ peptide fused to photoactivable mCherry (KFERQ-PA-mCherry), has recently been shown to localize in the late endosome and lysosome compartment in larval fat body upon prolonged starvation, an effect dependent on Hsc70-4, the fly ortholog of HSPA8, and the ESCRT (endosomal sorting complexes required for transport)

machinery [14]. This was interpreted as an evidence of eMI rather than CMA. We therefore used this biosensor to probe for the effect of LAMP2A on the accumulation of fluorescent puncta in late endosomes and lysosomes, either in fed or starvation conditions [14]. Although we observed an increase in biosensor puncta per cell in the larval fat body upon LAMP2A expression under fed conditions in some experiments, the effect was found not to be significant when all data were pooled (Fig. 3Ai-ii' and B). Starvation increased sensor puncta formation, as previously reported [14], but not further in LAMP2A-expressing larvae (Fig. 3Aiii-iv' and B). Similar results were obtained with another eMI biosensor, KFERQ-Split-Venus [13], in which the KFERQ recognition motif was fused to both the N- and C-terminal part of the yellow fluorescent protein variant Venus [63]. Split-Venus reconstitution occurs when both moieties concentrate upon endosomal targeting, leading to a fluorescent signal [13]. In the larval fat body, LAMP2A expression did not increase Split-Venus fluorescence nor puncta formation under fed or starvation conditions (Fig. S3A-C). Therefore, LAMP2A expression does not seem to induce KFERQ-dependent autophagy efficiently in the larval fat body.

To examine the effect of LAMP2A expression on selective autophagy in the brain, we expressed N- and C- KFERQ-Split-Venus together in all neurons, either with or without LAMP2A. Brains from fed or starved adult flies were dissected and mounted for confocal microscopy. Representative scans of whole brains are shown in Fig. S4A. Fluorescent puncta were detected in the neuropil at high resolution, in particular in the calyx region of the mushroom bodies, where they could be most easily visualized and quantified (Fig. 3C and Fig. S4B). These puncta likely represent Split-Venus reconstitution events in the late endosome and lysosome compartments. A small but significant increase in overall fluorescence intensity in the brain

neuropil of fed flies was observed at low resolution when LAMP2A was coexpressed (Fig. 3D). We observed, remarkably, that the number of puncta in the calyx region was strongly increased (about twice as much) compared to controls without LAMP2A (Fig. 3E). In contrast, we could not see significant puncta increments under starvation condition (Fig. 3D and E). This suggests that human LAMP2A can promote KFERQ motif-dependent selective autophagy in the fly nervous system. However, this effect does not occur in all tissues and has not been observed under starvation.

***LAMP2A upregulates Atg5 expression and enhances macroautophagy in fly neurons***

Suppression of macroautophagy in various models promotes neurodegeneration associated to the accumulation of polyubiquitinated protein aggregates [35,64-67]. Moreover, increasing basal macroautophagy is known to protect *Drosophila* against the deleterious consequences of oxidative stress [35,65,68]. We therefore considered macroautophagy as an alternative degradation process by which human LAMP2A could mediate neuroprotection. ATG5 is an E3-like ligase that together with ATG12 and ATG16L1 constitutes an elongation complex required for the formation of autophagosomes [69]. Here we found by western blot analysis that LAMP2A expression in neurons considerably increased levels of *Drosophila* Atg5 protein and of the Atg12-Atg5 complex (Fig. 4A and B). Because it has recently been reported that Atg5 inactivation induces locomotor defects in flies [44], the upregulation of Atg5 expression could in part explain the improvement in locomotion ability we observed upon LAMP2A expression in PD-like conditions and in aged wild-type flies.

Ref(2)P, the *Drosophila* ortholog of human SQSTM1/p62 (sequestosome 1), is an autophagosome cargo protein contributing to the clearance of ubiquitinated proteins [66,67,70], which is commonly used as a marker of autophagic flux in fly tissues [71]. Dopaminergic neurons are the primary target of paraquat in *Drosophila* [72]. We therefore compared anti-Ref(2)P immunostaining in brains of oxidative stress-challenged flies expressing or not expressing human LAMP2A in dopaminergic neurons. Whereas paraquat exposure increased Ref(2)P accumulation in neurons of control flies (Fig. 4Ci-ii and D), this effect was strikingly reduced upon LAMP2A expression (Fig. 4Ciii-iv and D). This indicates that human LAMP2A prevents paraquat-induced accumulation of Ref(2)P-containing aggregates in *Drosophila* neurons, most likely by enhancing clearance of these aggregates through Atg5-dependent macroautophagy. Recruitment of Atg8a/LC3, the major *Drosophila* ortholog of human GABARAP (GABA type A receptor associated protein) and MAP1LC3/LC3 (microtubule associated protein 1 light chain 3) ortholog families of yeast Atg8, during autophagosome assembly is an essential step in the macroautophagy process [73,74]. To search for a direct demonstration that LAMP2A increases autophagosome formation in fly neurons, we analyzed the density of Atg8a-positive puncta by immunostaining. As shown in Fig. 4E and F, we found that pan-neuronal expression of LAMP2A as a mean doubled the number of Atg8a-positive dots in the brain neuropil compared to control flies. This confirmed an expansion of the autophagosome compartment induced by LAMP2A expression in *Drosophila* neurons.

## Discussion

***Expression of the lysosomal receptor LAMP2A confers stress resistance and neuroprotection in* Drosophila**

The autophagy-lysosome pathway plays a fundamental role in cellular physiology. Impairment in this process, and particularly of macroautophagy and CMA, is often associated with the progression of neurodegenerative diseases, including PD [15,16,26,27,75-78]. These autophagic pathways are therefore major potential targets to improve the curative treatment of these neuropathologies. Selective protein degradation by CMA depends on the presence of a KFERQ peptide motif or related sequences in protein substrates [79]. These proteins individually interact with a complex containing the cytosolic chaperone HSPA8, the lysosomal membrane glycoprotein LAMP2A and other proteins, in which protein substrates are unfolded and translocated from the cytosol to the lysosomal lumen for degradation through LAMP2A [15,18]. Although CMA has been extensively characterized in mammals, it is currently considered that this process does not occur in invertebrates, including *Drosophila*. The only fly ortholog to human LAMP2A, named Lamp1, does not contain the amino-acid sequence present in the C-terminal tail of LAMP2A that is required for CMA, and it apparently does not form a complex with *Drosophila* Hsc70-4, the ortholog of human HSPA8 [13]. Another selective autophagy process, eMI, seems to be used instead in the fly [13,14]. eMI has been described in mammals as a process whereby endosomes engulf cytosolic material through the formation of multivesicular bodies that later fuse with lysosomes [8]. Cytosolic proteins bearing a KFERQ motif can be selectively targeted to this autophagy pathway by a LAMP2A-independent process that involves Hsc70-4 and the ESCRT machinery [8,13,14].

Here we investigated the potential activity of ectopically expressed human LAMP2A in *Drosophila*. We found that pan-neuronal expression of LAMP2A is harmless for behavior and survival, but rather is potently neuroprotective in flies, conferring increased resistance to various stresses: nutrient starvation, paraquat exposure, or mutant SNCA accumulation. A common feature shared by all these stressors is that they induce a significant rise in neuronal oxidative stress. LAMP2A appears therefore able to activate a powerful protective response preventing the deleterious consequences of ROS accumulation in the *Drosophila* nervous system, suggesting that this membrane protein can stimulate autophagic mechanisms in this organism.

***LAMP2A expression in flies delays locomotor aging and SNCA-induced defects***

Impairment of intracellular proteolysis with age could be largely responsible for the deficient removal of oxidized proteins in old organisms [80]. We observed that neuronal LAMP2A expression significantly improved the locomotor performance of aging flies without modifying *Drosophila* lifespan. This suggests that preventing the accumulation of oxidized or damaged proteins can prolong healthspan but is not sufficient to increase longevity in *Drosophila*. As mentioned above, these results agree with reports in other models suggesting that a lower cellular oxidative stress during aging cannot by itself promote prolonged lifespan [81,82]. It is suspected that other age-related genetic and physiological processes, which are still largely unresolved, play a more decisive role in lifespan regulation [83].

In humans, PD pathogenesis is associated with CMA impairments in the substantia nigra [50,51] and this may contribute to SNCA accumulation and neurotoxic effects in this disease. PD-

303 associated SNCA and LRRK2 mutant proteins disrupt CMA-mediated cytosolic protein
304 degradation [26,27], leading to the accumulation of SNCA oligomers and other damaged and
305 potentially toxic proteins. Here we show in the *Drosophila* model that LAMP2A not only
306 protected against SNCA-induced locomotor impairments, but also reduced ROS and MDA
307 accumulation and so likely oxidative cellular damages, and at the same time decreased mutant
308 SNCA protein level. Such a potent protection is quite comparable to the positive effects of
309 virally-expressed LAMP2A against SNCA toxicity in the rat substantia nigra [28]. Our results
310 indirectly suggest that LAMP2A selectively activates clearance of the pathogenic aggregated
311 forms of $SNCA^{A30P}$ in *Drosophila* neurons, indicating again that an activation of autophagy is
312 involved in its neuroprotective effects.
313
314 ***LAMP2A induces a selective autophagy process in the fly brain***
315 We then assessed which type of autophagy can be activated by LAMP2A in *Drosophila*. It is
316 known that starvation first activates macroautophagy within 1 h of nutrient deprivation [34,84].
317 Prolonged starvation then triggers LAMP2A-dependent CMA in mammalian cells [85,86] or
318 ESCRT-dependent eMI in *Drosophila* [14]. Here we observed with 2 different eMI biosensors
319 that LAMP2A expression did not alter either fluorescence intensity or puncta formation in the
320 larval fat body under fed nor under starvation conditions. In contrast, when we expressed the
321 KFERQ-Split-Venus eMI sensor in the adult brain, we observed that LAMP2A induced a
322 significant increase in sensor fluorescence and puncta formation in fed but not in starved flies.
323 This suggests that LAMP2A can induce a form of selective autophagy in the fly brain, but that
324 this effect is unlikely to be involved in the increased starvation resistance induced by neuronal

expression of this human protein. In mammals, CMA can be induced by overexpression of its receptor LAMP2A [28,39]. As mentioned above, CMA is not expected to occur in *Drosophila* owing to the lack of a LAMP2A counterpart in invertebrates [13,14]. However, other key CMA partners are expressed such as Hsc70-4 that shares 87% identity with human HSPA8 [13], and a KFERQ-like motif is present in about 43% of the fly proteins [14]. Further work is needed, therefore, to determine whether human LAMP2A can induce a CMA-like process in the *Drosophila* brain.

### ***Human LAMP2A upregulates Atg5 and stimulates macroautophagy in* Drosophila**

Quite unexpectedly, we observed that human LAMP2A expression in fly neurons strongly increased levels of Atg5 and of the Atg12-Atg5 macroautophagy complex. This was apparently associated with an enhancement of autophagic flux because paraquat-induced Ref(2)P accumulation was prevented when LAMP2A was expressed. Finally, we observed that LAMP2A expression also markedly increased the density of Atg8a-positive puncta in the brain neuropil. Taken together, our results indicate that the ectopic expression of LAMP2A can increase autophagosome formation and enhance macroautophagy in flies. This is not contradictory to the effect we observed on LAMP2A-mediated clearance of mutant $SNCA^{A30P}$, as it has been shown that SNCA can be degraded either by CMA or macroautophagy in mammalian neurons [47]. Accordingly, it was recently reported that paraquat-induced oxidative stress or MPTP (1-methyl-4-phenyl-1,2,3,6-tetrahydropyridine) toxicity both impaired autophagic flux in human dopaminergic neuroblastoma cells and in zebrafish dopamine neurons, respectively, and that Atg5 appeared protective as well in these 2 PD models [68,87]. Our report also suggests a

potential inductive effect of LAMP2A on the expression or activity of autophagy-related proteins. A recent article indicated that the lack of *LAMP2* gene in mouse embryonic fibroblasts prevented STX17 (syntaxin 17) incorporation into autophagosomes, leading to a failure of their fusion with lysosomes [88], which is another indication that the LAMP2 proteins can contribute to autophagosome maturation.

In humans, *LAMP2* gene deficiency leads to Danon disease, histologically characterized by an extensive accumulation of autophagic vacuoles in various tissues and defects in the autophagosom and lysosome fusion process [21,89,90]. A similar apparent block of autophagy could be reproduced in *lamp2* knock-out mice, leading to the accumulation of autophagic vacuoles and of SQSTM1-positive aggregates in the brain [91-93], or by *LAMP2* inactivation in mouse and human cultured cells [88,94-96]. The *LAMP2* gene products appear to play a specific role in the fusion of autophagosomes with lysosomes [88,95,97]. A role for *LAMP2* in macroautophagy in human cells was also previously indicated by functional mapping [98]. However, the matter is not simple as *LAMP2* produces three protein isoforms with distinct roles in autophagy [19,21]. It would be therefore important to determine the respective function of these LAMP2 proteins in macroautophagy, possibly by comparing their neuroprotective effects in *Drosophila*. Our present study suggests that the human LAMP2A isoform can increase both KFERQ motif-dependent selective autophagy as well as macroautophagy in the fly brain. These effects could potentially reflect the diverse functions of this protein in the mammalian brain.

In future work, based on the highly positive effects of sustained LAMP2A expression reported here and the tractability of the *Drosophila* model, it should be possible to identify additional factors involved in LAMP2A-mediated neuroprotection. Such conserved factors or mechanisms

could represent novel therapeutic targets potentially useful to improve human health during aging and the treatment of PD and other degenerative diseases through autophagy activation.

## Materials and Methods

### Drosophila *culture and strains*

Flies were raised on a standard cornmeal-yeast-agar nutrient medium containing as an antifungal agent methyl 4-hydroxybenzoate (VWR International, 25605.293), at 25˚C and ~50% humidity with 12 h-12 h light-dark cycles. The following strains were used: $w^{1118}$ as wild-type control, *elav-Gal4* (*elav*$^{C155}$) from the Bloomington *Drosophila* Stock Center, *TH-Gal4* [99], *cg-Gal4* [100], *UAS-SNCA*$^{A30P}$ [40] (kindly provided by Mel Feany, Harvard Medical School, Boston, MA), *UAS-GFP::LAMP1*; *UAS-KFERQ-PA-mCherry* [14], *UAS-KFERQ-N-Venus*, *UAS-KFERQ-C- Venus* [13] (kindly provided by Patrik Verstreken, KU Leuven, Center for Human Genetic, Leuven, The Netherlands) and *UAS-LAMP2A* (this report). A strain carrying both *UAS-LAMP2A* and *UAS--SNCA*$^{A30P}$ on the second chromosome was generated by meiotic recombination. For purpose of simplification, we used the *driver>effector* convention to indicate genotypes: *elav-Gal4*; *UAS-LAMP2A* flies, for example, were denoted as *elav>LAMP2A*.

### *DNA constructs*

The human *LAMP2A* cDNA (clone H05D091G15) was obtained from Kabushiki Kaisha DNAFORM. The 1250 base pair *LAMP2A* insert was PCR amplified using primers with added restriction sites (Table S1). The sequence upstream of the ATG initiation codon in the forward primer was modified to match the *Drosophila* translation start consensus sequence. The PCR fragment was inserted into pUAST [101] and verified by sequencing (GATC Biotech). The *UAS-LAMP2A* plasmid

was sent to BestGene Inc. for P-element transformation by random insertion. Non-recessive lethal second- and third-chromosome insertions that yielded strong expression were selected and used thereafter.

***RNA detection***

RT-PCR analysis was carried out and analyzed as previously described [72]. Total RNA was isolated by standard procedure generally from 20 heads of 10-day-old flies collected on ice and lysed in 600 µl QIAzol Reagent (Qiagen, 79306). Total RNA (1 µg) was reverse transcribed using oligo(dT) primers with Maxima First Strand cDNA Synthesis Kit (Thermo Fisher Scientific, K1671). Approximately 1 ng of the first strand cDNA was amplified in 25 µl of reaction mixture using PrimeStar Max DNA polymerase (Takara Bio, R045A). The program cycles included 10 s denaturation at 98°C, 10 s annealing at 55°C and 30 s elongation at 72°C, repeated 25 to 35 times. PCR product levels were estimated after electrophoresis by densitometry with the Fiji software [102]. Data were normalized to amplification level of the ribosomal *RpL32*/*rp49* transcript. Sequences of the primers used are indicated in Table S2.

***Adult brain immunostaining***

Whole-mount brains from adult flies aged 8 days a.E. were dissected and processed for immunostaining as previously described [43,72]. The primary antibodies were: mouse monoclonal anti-human LAMP2 used at 1:200 dilutions (Developmental Studies Hybridoma Bank, H4B4), rabbit polyclonal antibody against *Drosophila* Ref(2)P [103] used at 1:100 (kindly provided by Sébastien Gaumer, Université Versailles-St-Quentin-en-Yvelines, France) and mouse monoclonal anti-human GABARAP (anti-Atg8) used at 1:500 (Santa Cruz Biotechnology, sc-377300). Note that the amino acid sequences of human GABARAP and *Drosophila* Atg8a shares

92% identity and we also checked by western blot that this GABARAP antibody that cross-reacts with multiple species recognizes *Drosophila* Atg8a. Brains were mounted in Prolong Gold Antifade Mountant (Thermo Fisher Scientific, P36930) and images were acquired on a Nikon A1R confocal microscope (Nikon Instruments, Tokyo, Japan). Laser, filter and gain settings remained constant within each experiment. The number of Atg8a particles was scored after selecting the area of interest by using the particle analysis tool of the Fiji software.

***Starvation and oxidative stress resistance***

To monitor starvation resistance, 10-day-old female *Drosophila* were kept in vials containing Whatman blotting paper (Sigma-Aldrich, WHA3001917) soaked with water and no nutrient medium. Dead flies were scored every 12 h. At least 100 flies were tested per genotype. Oxidative stress resistance was assayed by exposure to paraquat (methyl viologen dichloride hydrate; Sigma-Aldrich, 856177) using a previously described dietary ingestion procedure [72]. Non-virgin 8-day-old female *Drosophila (*~100 per genotype) were starved for 2 h in empty vials. They were then exposed to 20 mM paraquat diluted in 2% (wt:vol) sucrose (Euromedex, 200-301-B) (or sucrose only for controls) in 2-inch (5.2 cm) diameter Petri dishes (10 flies per dish) containing 2 layers of Whatman blotting paper (Sigma-Aldrich, WHA3001917) soaked with the paraquat solution and incubated at 25°C in saturating humidity conditions. Fly survival was scored after 24, 48 and 72 h. In some experiments, brains from flies exposed to 20 mM paraquat for 24h were dissected and processed for immunostaining.

***Locomotion assay***

Locomotor decline during aging was monitored by a SING test as previously described [42,45]. For each genotype, 50 adult males divided into 5 groups of 10 flies were placed in a vertical

column (25-cm long, 1.5-cm diameter) with a conic bottom end and left for approximately 25 min for habituation. They were tested individually by gently tapping them down (startle), and scoring the number of flies having reached the top of the column (above 22 cm) and remaining at the bottom end (below 4 cm) after 1 min. Each group was assayed 3 times at 15 min intervals. The performance index for each column was calculated as follows: $½[1 + (n_{top}-n_{bot})/n_{tot}]$, where $n_{tot}$ is the total number of flies, and $n_{top}$ and $n_{bot}$ the number of flies at the top and at the bottom, respectively. Results are the mean and SEM of the scores obtained with the 5 groups of flies per genotype.

***Longevity studies***

Lifespan analysis was performed as described [43]. *Drosophila* adult males (~50 animals/bottle in triplicate for each genotype) were collected within 24 h of emergence and incubated at 25°C. They were transferred into fresh bottles or vials every 2 or 3 days and the number of surviving flies was scored. Data are expressed as percentage of the initial fly number as a function of time.

***Fluorescent biosensors***

To monitor eMI activity in larvae, we first used a fluorescent sensor containing a KFERQ motif fused to photoactivable mCherry (KFERQ-PA-mCherry) as previously described [14]. Briefly, *cg-Gal4*, *UAS-GFP::LAMP-1*; *UAS-KFERQ-PA-mCherry* virgins were mated to $w^{1118}$ or *UAS-LAMP2A* males. Early 3$^{rd}$ instar progeny larvae of these crosses were photoactivated and then incubated for 25h on 20% sucrose with heat-killed yeast paste for fed conditions, or 20% sucrose only for starvation. Following which, they were cut open, fixed in 4% paraformaldehyde (VWR International, 100503-917), and processed for fat body tissue imaging on an ApoTome.2 system

(Carl-Zeiss, Oberkochen, Germany). Around 150 cells were quantified in total per genotype in 4 independent experiments.

In other sets of experiments, we have used a Split-Venus eMI sensor [13], in which the recognition motif KFERQ is fused both to the N- or C-terminal portion of the yellow fluorescent protein variant Venus [63]. Split-Venus reconstitution occurs when both moieties concentrate upon eMI targeting, leading to a fluorescent signal [13]. *UAS-KFERQ-N-Venus*, *UAS-KFERQ-C-Venus* (here named *UAS-KFERQ-Split-Venus-NC*, control) or recombined *UAS-KFERQ-Split-Venus-NC*, *UAS-LAMP2A* flies were crossed to *cg-Gal4* or *elav-Gal4* for expression in fat body cells or in all neurons, respectively. 3$^{rd}$ instar larvae (3 to 5 per genotype in each experiment) were either fed on 20% sucrose plus yeast paste or starved for 4 h on 20% sucrose, before being processed for fat body tissue imaging. Whole-mount brains (3 to 7 per genotype and feeding condition in each experiment) were dissected from progeny adults aged 7 to 10 days a.E that were either normally fed or starved for 24 h. Brains were then fixed in 4% paraformaldehyde for 20 min and washed in 1X phosphate-buffered saline (PBS) pH 7.4 (Thermo Fisher Scientific, 70011044) for 15 min, twice. Split-Venus reconstitution in tissues was monitored by yellow fluorescence imaging (excitation at 515 nm, emission at 528 nm) on a Nikon A1R confocal microscope. Laser, filter and gain settings remained constant within one experiment. Overall fluorescence intensity was determined with the Fiji software by measuring relative mean density on Z projections of portions of fat body or on the whole brain, respectively, and the data were normalized to respective control values. The number of puncta was scored after selecting the area of interest by using the particle analysis tool of the Fiji software. Results are mean ± SEM of 3 independent experiments.

***Western blot analyses***

Fly heads (20) were homogenized in 100 µl RIPA buffer (Sigma-Aldrich, R0278) containing protease inhibitors (cOmplete mini Protease Inhibitor Cocktail tablets; Roche Diagnostics, 11836153001) using a Minilys apparatus (Bertin Instruments, Montigny-le-Bretonneux, France). The lysates were incubated on ice for 30 min and centrifuged at 8,000 g for 10 min at 4°C. Protein samples were prepared by diluting the supernatant in 1 x final NuPAGE LDS Sample Buffer (Thermo Fisher Scientific, NP0001) and reducing agent (Thermo Fisher Scientific, NP0009), followed by 10-min denaturation at 70°C and 5 s centrifugation at 1,000 g. Proteins were separated in 4-12% NuPAGE Bis-Tris precast polyacrylamide gels (Thermo Fisher Scientific, NP0321BOX), using PageRuler Plus Prestained Protein Ladder (Thermo Fisher Scientific, 26619) as migration marker, and electrotransferred to Hybond ECL nitrocellulose (GE Healthcare Life Sciences, RPN3032D) or Amersham Hybond P 0.45 PVDF membranes (GE Healthcare Life Sciences, 10600023). Membranes were blocked after transfer for 2 h at room temperature in 1X Tris-buffered saline (TBS) pH 7.4 (Thermo Fisher Scientific, 10648973) containing 0.05% (v/v) Tween 20 (Sigma Aldrich, P1379) (TBS-Tween) supplemented with 5% skim milk. For immunodetection of human SNCA, transferred membranes were first fixed with 0.4% paraformaldehyde in PBS for 30 min to prevent the detachment of SNCA monomers as recently described [104]. The fixed membranes were then washed in TBS-Tween 3 times for 10 min and blocked for 2 h at room temperature in TBS-Tween + 5% skim milk. Membranes were then incubated overnight at 4°C in TBS-Tween containing 1% (w/v) bovine serum albumin (Euromedex, 04-100-812-C) with the following primary antibodies: rabbit polyclonal anti-SNCA used at 1:1,000 dilutions (Sigma-Aldrich, S3062), rabbit polyclonal anti-Atg5 at 1:500 (Novus

Biologicals, NB110-53818) and mouse monoclonal anti-ACTB (actin beta) at 1:5,000 (Abcam, ab20272) that cross-reacts with *Drosophila* Act5C (Actin 5C). Membranes were washed three times for 10 min in TBS-Tween and then incubated for 2 h at room temperature with horseradish peroxidase (HRP)-conjugated anti-rabbit (Abcam, ab7132) or anti-mouse (Jackson ImmunoResearch, 115-035-146) secondary antibodies at 1:5,000. Immunolabeled bands were revealed by using ECL RevelBlOt Intense (Ozyme, OZYB002-1000) as chemiluminescent HRP substrate and digitally acquired at different exposure times using ImageQuant TL software (GE Healthcare Life Science, Chicago, USA). Densitometry measures were made using Fiji software and normalized to Act5C measures as internal controls.

***ROS detection and quantification***

Reactive oxygen species (ROS) level was determined with the fluorescent dye dihydroethidium (DHE) (Thermo Fisher Scientific, D11347) following a published protocol [105] adapted to whole-mount *Drosophila* brains. DHE is preferentially oxidized by superoxide ($O_2^{\bullet-}$) but it is also sensitive to other ROS, such as $H_2O_2$ and $^{\bullet}OH$, producing bright-red fluorescent products (ethidium, 2-hydroxyethidium, and dimers) measured at 555 nm as an index of intracellular oxidant formation [106]. 5 to 8 adult brains per genotype were dissected in Schneider insect medium (Sigma Aldrich, S0146) and incubated on an orbital shaker for 10 min at room temperature in 30 µM DHE diluted in the same medium. The brains were then washed 3 times in Schneider medium and fixed for 6 min in 7% formaldehyde (Thermo Fisher Scientific, 28908) in PBS. After rinsing in PBS and mounting in Vectashield Antifade Mounting Medium (Vector Laboratories, H-1000), the brains were immediately scanned at constant gain setting on a

Nikon A1R confocal microscope. Relative ROS levels were measured by quantification of whole brain average intensity level of the dye fluorescence using the Fiji software.

***Estimation of lipid peroxidation***

The quantification of MDA is an index of lipid peroxidation and ROS-induced damage [59]. MDA was determined in *Drosophila* brain extracts using a described procedure [107]. Ten brains were homogenized in 200 µl of ice-cold 20 mM Tris-HCl (Euromedex, EU0011C) (5 replicates of 10 brains per genotype) using a Minilys apparatus (Bertin Instruments, Montigny-le-Bretonneux, France) and the homogenate was microcentrifuged at 3,000 g for 20 min at 4°C. Then, 1 µl of the supernatant was added to 1.3 ml of acetonitrile-methanol 3:1 (vol:vol) solution containing 7.7 mM 1-methyl-2-phenylindole (Sigma Aldrich, 404888) and 0.3 ml of 37% HCl was added. After vortexing, the tubes were incubated at 45°C for 40 min, cooled on ice and microcentrifuged at 1,500 g for 10 min at 4°C. Optical density of the supernatants was measured at 586 nm.

***Statistical analysis***

Data from locomotor assays and oxidative stress resistance have been analyzed by one-way ANOVA with the post-hoc Tukey-Kramer test. Survival curves for starvation resistance and longevity experiments were generated and compared using the log-rank test. Statistical analysis of DHE, MDA and eMI biosensor quantifications was performed by the Student t-test or one-way ANOVA with Tukey pairwise comparisons. All statistical analyses were performed with the Prism 6 software (GraphPad Software, San Diego, California). Significant values in all figures: $*p<0.05$, $**p<0.01$, $***p<0.001$.

## Acknowledgements

We thank Drs. Mel Feany and Patrik Verstreken for *Drosophila* stocks, Dr. Sébastien Gaumer for antibody samples and Dr. Giorgio Matassi for helpful discussion about LAMP2A phylogenetics. This work was supported by funding from the Fondation de France, Association France-Parkinson, PSL Research University and Labex MemoLife (ANR-10-LABX-54 MEMOLIFE) to SB and NIH R01 GM119160 to AJ. ARI was recipient of a PhD fellowship from the Doctoral school 3C (ED3C) at University Pierre-et-Marie Curie, Paris, and then supported by a postdoctoral salary from the Labex MemoLife. JS, CP and AD are supported by PhD fellowships from the Chinese Scholarship Council, Association Lesch-Nyhan Action, and PSL Research University, respectively.

## References


[1] Boya P, Reggiori F, Codogno P. Emerging regulation and functions of autophagy. Nat Cell Biol. 2013;15(7):713–720.

[2] Parzych KR, Klionsky DJ. An overview of autophagy: morphology, mechanism, and regulation. Antioxid Redox Signal. 2014;20(3):460–473.

[3] Menzies FM, Fleming A, Rubinsztein DC. Compromised autophagy and neurodegenerative diseases. Nat Rev Neurosci. 2015;16(6):345–57.

[4] Bento CF, Renna M, Ghislat G, et al. Mammalian autophagy: how does it work? Annu Rev Biochem. 2016;85:685–713.

[5] Feng Y, He D, Yao Z, et al. The machinery of macroautophagy. Cell Res. 2014;24(1):24–41.

[6] Ktistakis NT, Tooze SA. Digesting the expanding mechanisms of autophagy. Trends Cell Biol. 2016;26(8):624–635.

[7] Mijaljica D, Prescott M, Devenish RJ. Microautophagy in mammalian cells: revisiting a 40-year-old conundrum. Autophagy. 2011;7(7):673–682.

[8] Sahu R, Kaushik S, Clement CC, et al. Microautophagy of cytosolic proteins by late endosomes. Dev Cell. 2011;20(1):131–139.

[9] Kawamura N, Sun-Wada G-H, Aoyama M, et al. Delivery of endosomes to lysosomes via microautophagy in the visceral endoderm of mouse embryos. Nat Commun. 2012;3:1071.

[10] Dice JF. Peptide sequences that target cytosolic proteins for lysosomal proteolysis. Trends Biochem Sci. 1990;15(8):305–309.

[11] Agarraberes FA, Dice JF. A molecular chaperone complex at the lysosomal membrane is required for protein translocation. J Cell Sci. 2001;114(13):2491–2499.

[12] Horst M, Knecht EC, Schu PV. Import into and degradation of cytosolic proteins by isolated yeast vacuoles. Mol Biol Cell. 1999;10(9):2879–2889.

[13] Uytterhoeven V, Lauwers E, Maes I, et al. Hsc70-4 deforms membranes to promote synaptic protein turnover by endosomal microautophagy. Neuron. 2015;88(4):735–748.

[14] Mukherjee A, Patel B, Koga H, et al. Selective endosomal microautophagy is starvation-inducible in *Drosophila*. Autophagy. 2016; 12(11):1984–1999.

[15] Cuervo AM, Wong E. Chaperone-mediated autophagy: roles in disease and aging. Cell

Res. 2014;24(1):92–104.

[16] Wang G, Mao Z. Chaperone-mediated autophagy: roles in neurodegeneration. Transl Neurodegener. 2014;3:20.

[17] Xilouri M, Stefanis L. Chaperone mediated autophagy in aging: starve to prosper. Ageing Res Rev. 2016;32:13-21.

[18] Cuervo AM, Dice JF. A receptor for the selective uptake and degradation of proteins by lysosomes. Science. 1996;273(5274):501–503.

[19] Eskelinen E-L, Cuervo AM, Taylor MRG, et al. Unifying nomenclature for the isoforms of the lysosomal membrane protein LAMP-2. Traffic. 2005;6(11):1058–1061.

[20] Wilke S, Krausze J, Büssow K. Crystal structure of the conserved domain of the DC lysosomal associated membrane protein: implications for the lysosomal glycocalyx. BMC Biol. 2012;10:62.

[21] Endo Y, Furuta A, Nishino I. Danon disease: a phenotypic expression of LAMP-2 deficiency. Acta Neuropathol. 2015;129(3):391–398.

[22] Cuervo AM, Dice JF. Unique properties of lamp2a compared to other lamp2 isoforms. J Cell Sci. 2000;113(24):4441–4450.

[23] Qi L, Zhang X-D. Role of chaperone-mediated autophagy in degrading Huntington's disease-associated huntingtin protein. Acta Biochim Biophys Sin (Shanghai). 2014;46(2):83–91.

[24] Xilouri M, Stefanis L. Chaperone mediated autophagy to the rescue: A new-fangled target for the treatment of neurodegenerative diseases. Mol Cell Neurosci. 2015;66(A):29–36.

[25] Cai Z, Zeng W, Tao K, E Z, et al. Chaperone-mediated autophagy: roles in neuroprotection. Neurosci Bull. 2015;31(4):452–458.

[26] Cuervo AM, Stefanis L, Fredenburg R, et al. Impaired degradation of mutant alpha-synuclein by chaperone-mediated autophagy. Science. 2004;305(5688):1292–1295.

[27] Orenstein SJ, Kuo S-H, Tasset I, et al. Interplay of LRRK2 with chaperone-mediated autophagy. Nat Neurosci. 2013;16(4):394–406.

[28] Xilouri M, Brekk OR, Landeck N, et al. Boosting chaperone-mediated autophagy *in vivo* mitigates α-synuclein-induced neurodegeneration. Brain. 2013;136(7):2130–2146.

[29] Chang Y-Y, Neufeld TP. Autophagy takes flight in *Drosophila*. FEBS Lett. 2010;584(7):1342–1349.

[30] Mulakkal NC, Nagy P, Takats S, et al. Autophagy in *Drosophila*: from historical studies to current knowledge. Biomed Res Int. 2014;2014:273473.

[31] Nagy P, Varga Á, Kovács AL, et al. How and why to study autophagy in *Drosophila*: it's more than just a garbage chute. Methods. 2015;75:151–161.

[32] Zhang H, Baehrecke EH. Eaten alive: novel insights into autophagy from multicellular model systems. Trends Cell Biol. 2015;25(7):376–387.

[33] Tracy K, Baehrecke EH. The role of autophagy in *Drosophila* metamorphosis. Curr Top Dev Biol. 2013;103:101–25.

[34] Scott RC, Schuldiner O, Neufeld TP. Role and regulation of starvation-induced autophagy in the *Drosophila* fat body. Dev Cell. 2004;7(2):167–178.

[35] Simonsen A, Cumming RC, Brech A, et al. Promoting basal levels of autophagy in the nervous system enhances longevity and oxidant resistance in adult *Drosophila*. Autophagy. 2008;4(2):176–184.

[36] Demontis F, Perrimon N. FOXO/4E-BP signaling in *Drosophila* muscles regulates organism-wide proteostasis during aging. Cell. 2010;143(5):813–825.

[37] Filomeni G, De Zio D, Cecconi F. Oxidative stress and autophagy: the clash between damage and metabolic needs. Cell Death Differ. 2015;22(3):377–388.

[38] Kiffin R, Christian C, Knecht E, et al. Activation of chaperone-mediated autophagy during oxidative stress. Mol Biol Cell. 2004;15(11):4829–4840.

[39] Zhang C, Cuervo AM. Restoration of chaperone-mediated autophagy in aging liver improves cellular maintenance and hepatic function. Nat Med. 2008;14(9):959–965.

[40] Feany MB, Bender WW. A *Drosophila* model of Parkinson's disease. Nature. 2000;404(6776):394–398.

[41] Jones MA, Grotewiel M. *Drosophila* as a model for age-related impairment in locomotor and other behaviors. Exp Gerontol. 2011;46(5):320–325.

[42] Riemensperger T, Issa A-R, Pech U, et al. A single dopamine pathway underlies progressive locomotor deficits in a *Drosophila* model of Parkinson disease. Cell Rep. 2013;5(4):952–960.

[43] Riemensperger T, Isabel G, Coulom H, et al. Behavioral consequences of dopamine deficiency in the *Drosophila* central nervous system. Proc Natl Acad Sci USA. 2011; 108(2):834–839.

[44] Kim M, Sandford E, Gatica D, et al. Mutation in ATG5 reduces autophagy and leads to

ataxia with developmental delay. Elife. 2016;5:e12245.

[45] Vaccaro A, Issa A-R, Seugnet L, et al. *Drosophila* clock is required in brain pacemaker neurons to prevent premature locomotor aging independently of its circadian function. PLoS Genet. 2017;13(1):e1006507.

[46] Dehay B, Bourdenx M, Gorry P, et al. Targeting α-synuclein for treatment of Parkinson's disease: mechanistic and therapeutic considerations. Lancet Neurol. 2015;14(8):855–866.

[47] Vogiatzi T, Xilouri M, Vekrellis K, et al. Wild type alpha-synuclein is degraded by chaperone-mediated autophagy and macroautophagy in neuronal cells. J Biol Chem. 2008;283(35):23542–23556.

[48] Mak SK, McCormack AL, Manning-Bog AB, et al. Lysosomal degradation of alpha-synuclein *in vivo*. J Biol Chem. 2010;285(18):13621–13629.

[49] Malkus KA, Ischiropoulos H. Regional deficiencies in chaperone-mediated autophagy underlie α-synuclein aggregation and neurodegeneration. Neurobiol Dis. 2012;46(3):732–744.

[50] Alvarez-Erviti L, Seow Y, Schapira AHV, et al. Influence of microRNA deregulation on chaperone-mediated autophagy and α-synuclein pathology in Parkinson's disease. Cell Death Dis. 2013; 4(3):e545.

[51] Alvarez-Erviti L, Rodriguez-Oroz MC, Cooper JM, et al. Chaperone-mediated autophagy markers in Parkinson disease brains. Arch Neurol. 2010;67(12):1464–1472.

[52] Barone MC, Sykiotis GP, Bohmann D. Genetic activation of Nrf2 signaling is sufficient to ameliorate neurodegenerative phenotypes in a *Drosophila* model of Parkinson's disease. Dis Model Mech. 2011;4(5):701–707.

[53] Butler EK, Voigt A, Lutz AK, et al. The mitochondrial chaperone protein TRAP1 mitigates α-Synuclein toxicity. PLoS Genet. 2012;8(2):e1002488.

[54] Breda C, Nugent ML, Estranero JG, et al. Rab11 modulates α-synuclein-mediated defects in synaptic transmission and behaviour. Hum Mol Genet. 2015;24(4):1077–1091.

[55] Xu J, Kao S-Y, Lee FJS, et al. Dopamine-dependent neurotoxicity of alpha-synuclein: a mechanism for selective neurodegeneration in Parkinson disease. Nat Med. 2002;8(6):600–606.

[56] Botella JA, Bayersdorfer F, Schneuwly S. Superoxide dismutase overexpression protects dopaminergic neurons in a *Drosophila* model of Parkinson's disease. Neurobiol Dis. 2008;30(1):65–73.

[57] Alvarez-Fischer D, Fuchs J, Castagner F, et al. Engrailed protects mouse midbrain dopaminergic neurons against mitochondrial complex I insults. Nat Neurosci. 2011;14(10):1260–1266.

[58] Wang B, Liu Q, Shan H, et al. Nrf2 inducer and cncC overexpression attenuates neurodegeneration due to α-synuclein in *Drosophila*. Biochem Cell Biol. 2015;93(4):351–358.

[59] Del Rio D, Stewart AJ, Pellegrini N. A review of recent studies on malondialdehyde as toxic molecule and biological marker of oxidative stress. Nutr Metab Cardiovasc Dis. 2005;15(4):316–328.

[60] Hosamani R, Muralidhara. Acute exposure of *Drosophila melanogaster* to paraquat causes oxidative stress and mitochondrial dysfunction. Arch Insect Biochem Physiol. 2013;83(1):25–40.

[61] Cuervo AM, Dice JF. Regulation of lamp2a levels in the lysosomal membrane. Traffic 2000;1(7):570–583.

[62] Dohi E, Tanaka S, Seki T, et al. Hypoxic stress activates chaperone-mediated autophagy and modulates neuronal cell survival. Neurochem Int. 2012;60:431–42.

[63] Nagai T, Ibata K, Park ES, et al. A variant of yellow fluorescent protein with fast and efficient maturation for cell-biological applications. Nat Biotechnol. 2002;20(1):87–90.

[64] Komatsu M, Waguri S, Chiba T, al. Loss of autophagy in the central nervous system causes neurodegeneration in mice. Nature. 2006;441(7095):880–884.

[65] Juhász G, Erdi B, Sass M, et al. Atg7-dependent autophagy promotes neuronal health, stress tolerance, and longevity but is dispensable for metamorphosis in *Drosophila*. Genes Dev. 2007;21(23):3061–3066.

[66] Bartlett BJ, Isakson P, Lewerenz J, et al. p62, Ref(2)P and ubiquitinated proteins are conserved markers of neuronal aging, aggregate formation and progressive autophagic defects. Autophagy. 2011;7(6):572–583.

[67] Gupta VK, Scheunemann L, Eisenberg T, et al. Restoring polyamines protects from age-induced memory impairment in an autophagy-dependent manner. Nat Neurosci. 2013;16(10):1453–1460.

[68] Garcia-Garcia A, Anandhan A, Burns M. Impairment of Atg5-dependent autophagic flux promotes paraquat-and MPP+-induced apoptosis but not rotenone or 6-hydroxydopamine toxicity. Toxicol Sci. 2013;136(1):166–182.

[69] Kharaziha P, Panaretakis T. Dynamics of Atg5-Atg12-Atg16L1 aggregation and

deaggregation. Meth Enzymol. 2017;587:247–255.

[70] Komatsu M, Waguri S, Koike M, al. Homeostatic levels of p62 control cytoplasmic inclusion body formation in autophagy-deficient mice. Cell. 2007;131(6):1149–1163.

[71] DeVorkin L, Gorski SM. Monitoring autophagic flux using Ref(2)P, the *Drosophila* p62 ortholog. Cold Spring Harb Protoc. 2014;2014(9):959–966.

[72] Cassar M, Issa A-R, Riemensperger T, et al. A dopamine receptor contributes to paraquat-induced neurotoxicity in *Drosophila*. Hum Mol Genet. 2015;24(1):197–212.

[73] Xu T, Kumar S, Denton D. Characterization of autophagic responses in *Drosophila melanogaster*. Meth Enzymol. 2017;588:445–465.

[74] Lőrincz P, Mauvezin C, Juhász G. Exploring autophagy in *Drosophila*. Cells. 2017;6(3):22.

[75] Xilouri M, Vogiatzi T, Vekrellis K, et al. Abberant alpha-synuclein confers toxicity to neurons in part through inhibition of chaperone-mediated autophagy. PLoS ONE. 2009;4(5):e5515.

[76] Liu X, Huang S, Wang X, Tang B, Li W, Mao Z. Chaperone-mediated autophagy and neurodegeneration: connections, mechanisms, and therapeutic implications. Neurosci Bull. 2015;31(4):407–415.

[77] Frake RA, Ricketts T, Menzies FM, et al. Autophagy and neurodegeneration. J Clin Invest. 2015;125(1):65–74.

[78] Martini-Stoica H, Xu Y, Ballabio A, et al. The autophagy-lysosomal pathway in neurodegeneration: a TFEB perspective. Trends Neurosci. 2016;39(4):221–234.

[79] Dice JF. Chaperone-mediated autophagy. Autophagy. 2007;3(4):295–299.

[80] Vanhooren V, Navarrete Santos A, Voutetakis K, et al. Protein modification and maintenance systems as biomarkers of ageing. Mech Ageing Dev. 2015;151:71–84.

[81] Jang YC, Pérez VI, Song W, et al. Overexpression of Mn superoxide dismutase does not increase life span in mice. J Gerontol A Biol Sci Med Sci. 2009;64(11):1114–1125.

[82] Van Raamsdonk JM, Hekimi S. Deletion of the mitochondrial superoxide dismutase sod-2 extends lifespan in *Caenorhabditis elegans*. PLoS Genet. 2009;5(2):e1000361.

[83] Gems D, Partridge L. Genetics of longevity in model organisms: debates and paradigm shifts. Annu Rev Physiol. 2013;75:621–644.

[84] Rusten TE, Lindmo K, Juhász G, et al. Programmed autophagy in the *Drosophila* fat body is induced by ecdysone through regulation of the PI3K pathway. Dev Cell. 2004;7(2):179–192.

[85] Cuervo AM, Knecht E, Terlecky SR, et al. Activation of a selective pathway of lysosomal proteolysis in rat liver by prolonged starvation. Am J Physiol. 1995;269(5-1):C1200–C1208.

[86] Massey AC, Kaushik S, Sovak G, et al. Consequences of the selective blockage of chaperone-mediated autophagy. Proc Natl Acad Sci USA. 2006;103(15):5805–5810.

[87] Hu Z-Y, Chen B, Zhang J-P, et al. Up-regulation of autophagy-related gene 5 (ATG5) protects dopaminergic neurons in a zebrafish model of Parkinson's disease. J Biol Chem. 2017;292(44):18062–18074.

[88] Hubert V, Peschel A, Langer B, et al. LAMP-2 is required for incorporating syntaxin-17 into autophagosomes and for their fusion with lysosomes. Biol Open. 2016;5(10):1516–1529.

[89] Nishino I, Fu J, Tanji K, et al. Primary LAMP-2 deficiency causes X-linked vacuolar cardiomyopathy and myopathy (Danon disease). Nature. 2000;406(6798):906–910.

[90] Rowland TJ, Sweet ME, Mestroni L, et al. Danon disease - dysregulation of autophagy in a multisystem disorder with cardiomyopathy. J Cell Sci. 2016;129(11):2135–2143.

[91] Tanaka Y, Guhde G, Suter A, et al. Accumulation of autophagic vacuoles and cardiomyopathy in LAMP-2-deficient mice. Nature. 2000;406(6798):902–906.

[92] Saftig P, Beertsen W, Eskelinen E-L. LAMP-2: a control step for phagosome and autophagosome maturation. Autophagy. 2008;4(4):510–512.

[93] Rothaug M, Stroobants S, Schweizer M, et al. LAMP-2 deficiency leads to hippocampal dysfunction but normal clearance of neuronal substrates of chaperone-mediated autophagy in a mouse model for Danon disease. Acta Neuropathol Commun. 2015;3(1):6.

[94] Eskelinen E-L, Illert AL, Tanaka Y, et al. Role of LAMP-2 in lysosome biogenesis and autophagy. Mol Biol Cell. 2002;13:3355–3368.

[95] González-Polo R-A, Boya P, Pauleau A-L, et al. The apoptosis/autophagy paradox: autophagic vacuolization before apoptotic death. J Cell Sci. 2005;118:3091–3102.

[96] Morell C, Bort A, Vara-Ciruelos D, et al. Up-regulated expression of LAMP2 and autophagy activity during neuroendocrine differentiation of prostate cancer LNCaP cells. PLoS ONE. 2016;11:e0162977.

[97] Huynh KK, Eskelinen E-L, Scott CC, et al. LAMP proteins are required for fusion of lysosomes with phagosomes. EMBO J. 2007;26:313–324.

[98] Huttenhower C, Haley EM, Hibbs MA, et al. Exploring the human genome with

functional maps. Genome Res. 2009;19:1093–1106.

[99] Friggi-Grelin F, Coulom H, Meller M, et al. Targeted gene expression in Drosophila dopaminergic cells using regulatory sequences from tyrosine hydroxylase. J Neurobiol. 2003;54:618–27.

[100] Hennig KM, Colombani J, Neufeld TP. TOR coordinates bulk and targeted endocytosis in the *Drosophila melanogaster* fat body to regulate cell growth. J Cell Biol. 2006;173:963–974.

[101] Brand AH, Perrimon N. Targeted gene expression as a means of altering cell fates and generating dominant phenotypes. Development. 1993;118:401–15.

[102] Schindelin J, Arganda-Carreras I, Frise E, et al. Fiji: an open-source platform for biological-image analysis. Nat Methods. 2012;9:676–682.

[103] Nezis IP, Simonsen A, Sagona AP, et al. Ref(2)P, the *Drosophila melanogaster* homologue of mammalian p62, is required for the formation of protein aggregates in adult brain. J Cell Biol. 2008;180:1065–1071.

[104] Sasaki A, Arawaka S, Sato H, et al. Sensitive western blotting for detection of endogenous Ser129-phosphorylated α-synuclein in intracellular and extracellular spaces. Sci Rep. 2015;5:14211.

[105] Owusu-Ansah E, Yavari A, Banerjee U. A protocol for *in vivo* detection of reactive oxygen species. Protocol Exchange. 2008;doi:10.1038/nprot.2008.23.

[106] Zielonka J, Kalyanaraman B. Hydroethidine- and MitoSOX-derived red fluorescence is not a reliable indicator of intracellular superoxide formation: another inconvenient truth. Free Radic Biol Med. 2010;48:983–1001.

[107] Siddique YH, Mujtaba SF, Jyoti S, et al. GC-MS analysis of *Eucalyptus citriodora* leaf extract and its role on the dietary supplementation in transgenic *Drosophila* model of Parkinson's disease. Food Chem Toxicol. 2013;55:29–35.

## Figure Legends

**Figure 1.** The LAMP2A receptor promotes stress resistance and neuroprotection in *Drosophila*. (**A**) Starvation resistance. Expression of the human LAMP2A protein in all neurons significantly extended *Drosophila* survival upon prolonged starvation (*elav>LAMP2A* flies) compared to *elav-Gal4*/+ (*elav*/+) driver and *UAS-LAMP2A*/+ (*LAMP2A*/+) effector controls. (**B**) Paraquat exposure. Survival of *elav>LAMP2A* flies fed with 20 mM paraquat for 72 h was markedly increased compared to the *elav*/+ and *LAMP2A*/+ controls. (**C**) Effect on age-related locomotor decline. Pan-neuronal LAMP2A expression (*elav>LAMP2A* flies) significantly delayed age-related decrements in climbing performance (SING assay) compared to driver and effector controls that behaved like the wild type. (**D**) Lifespan assay. *elav*/+ and *elav>LAMP2A* flies showed similar longevity curves (median lifespan 57 and 55 days, respectively) indicating that neuronal LAMP2A expression does not affect *Drosophila* lifespan.

**Figure 2.** LAMP2A prevents SNCA-induced behavioral and oxidative defects in *Drosophila*. (**A**) LAMP2A coexpression fully prevented the progressive locomotor defects induced by pan-neuronal $SNCA^{A30P}$. Climbing ability (SING assay) of *elav>LAMP2A*, $SNCA^{A30P}$ flies was compared to that of *elav>*$SNCA^{A30P}$ and *elav>LAMP2A* flies at 10, 31 and 38 days after a.E. (**B**) Human LAMP2A reduced neuronal SNCA accumulation. Western blots of head protein extracts from 30-day-old *elav>*$SNCA^{A30P}$ flies compared to *elav>LAMP2A*, $SNCA^{A30P}$ probed with anti-SNCA antibody. Act5C was used as a loading control. Quantification of $SNCA^{A30P}$ protein level from 3 independent experiments. Coexpression of LAMP2A reduced $SNCA^{A30P}$ accumulation without

decreasing its mRNA level (see Fig. S2A). (**C**) Brain ROS levels in the brain of *elav>LAMP2A*, *SNCA*$^{A30P}$ flies were lower than those of *elav>SNCA*$^{A30P}$and comparable to the *elav*/+ control at both 2 and 30 days a.E. Representative pictures of DHE-labeled brain are shown in Fig. S2B. (**D**) MDA concentration assayed in the brain of 2- and 30-day-old adult *Drosophila* as an index of lipid peroxidation. Brain MDA level was markedly increased in *elav>SNCA*$^{A30P}$ flies but not in *elav>LAMP2A*, *SNCA*$^{A30P}$ flies that show similar levels as the *elav*/+ control.

**Figure 3.** Effect of LAMP2A on selective autophagy in the larval fat body and adult brain. (**A**) In 3rd-instar larval fat body cells, LAMP2A expression (*LAMP2A*, bottom panels) did not increase KFERQ-PA-mCherry fluorescent sensor puncta formation 25 h after photoactivation, either under fed (i, ii) or starvation (iii, iv) conditions, compared to controls (top panels). In composite images, mCherry fluorescence is in red and DAPI-stained nuclei are in blue. i'-iv' monochromatic images show the KFERQ-PA-mCherry single channel. Scale bars: 20 µm. (**B**) Quantification of puncta number per cell in larvae expressing photoactivated KFERQ-PA-mCherry in fat body with or without (control) LAMP2A under fed or starvation conditions. Starvation-induced sensor puncta formation was not further increased by LAMP2A expression. Similar results were obtained using a different eMI biosensor (KFERQ-Split-Venus) (shown in Fig. S3). (**C**) Localization of reconstituted KFERQ-Split-Venus sensor fluorescent puncta (arrowheads) in a posterior region of the adult brain of *elav>KFERQ-Split-Venus-NC* flies expressing the eMI sensor in all neurons. The square in the scheme (top inset) shows localization of the magnified brain region that surrounds the calyx of the mushroom body, where fluorescence was prominent and in which puncta were scored. Mb, mushroom body; Kc, cell bodies of the Mb Kenyon cells; ca,

calyx. Representative scans of whole brain and calyx region for the different genotypes and feeding conditions are shown in Fig. S4A and B, respectively. (**D, E**) Reconstitution of KFERQ-Split-Venus eMI sensor was increased in adult brain of fed, but not starved, flies expressing LAMP2A in all neurons (*elav>KFERQ-Split-Venus-NC*, *LAMP2A*) (*LAMP2A*, right panel), as indicated by higher overall fluorescence level (**D**) and increased density of eMI-positive puncta in the calyx region (**E**), compared to *elav>KFERQ-Split-Venus-NC* controls. Quantification from 3 independent experiments.

**Figure 4.** Human LAMP2A enhances macroautophagy in the *Drosophila* brain. (**A, B**) Effect of LAMP2A on Atg5 expression. (**A**) Western blot of head protein extracts from 10-day old control flies (*elav*/+) and flies expressing human LAMP2A in neurons (*elav>LAMP2A*) probed with anti-Atg5 antibody. LAMP2A expression markedly increased levels of Atg5 and of the Atg12-Atg5 complex that is required for autophagosome formation. Act5C served as a loading control. (**B**) Quantification of Atg5 protein and the Atg12-Atg5 complex from 3 independent western blot experiments. (**C, D**) Effect of LAMP2A on paraquat-induced Ref(2)P accumulation. (**C**) Anti-Ref(2)P immunostaining in whole-mount adult brains of *LAMP2A*/+ (panels i and ii) and *TH>LAMP2A* (panels iii and iv) flies exposed to paraquat (panels ii and iv) or not (panels i and iii). LAMP2A expression prevented paraquat-induced Ref(2)P accumulation (black puncta) suggesting that the human protein is able to maintain efficient autophagic flux under oxidative stress. Scale bar: 100 µm. (**D**) Quantification of Ref(2)P immunostaining in the central brain region normalized to *LAMP2A*/+ control not exposed to paraquat (n = 4 or 5 independent brains per condition). (**E, F**) Effect of LAMP2A on the number of Atg8a-positive puncta. (**E**) Anti-Atg8a

immunostaining in whole-mount adult brains of *elav*/+ (panel i) and *elav>LAMP2A* (panel ii) flies. The inset scheme on top shows the posterior neuropil region that was magnified in panels i and ii and in which Atg8a puncta were counted. Scale bars: 10 µm. (**F**) Quantification of Atg8a-positive dots. Each black circle (*elav*/+) or square (*elav>LAMP2A*) represents the score for a different brain. The number of Atg8a puncta that reflect autophagosome formation was markedly increased in LAMP2A-expressing flies. Similar results were obtained in 3 independent experiments.

## Supplementary figure legends

**Figure S1.** Expression of human LAMP2A in transgenic flies. (**A**) RT-PCR analysis performed on adult head RNAs detects *LAMP2A* mRNA in *elav>LAMP2A* flies and not in *elav-Gal4*/+ (*elav*/+) control. The tiny band amplified in the *UAS-LAMP2A/+* (*LAMP2A*/+) control could originate from a small amount of Gal4-independent transgene expression or genomic DNA contamination. Amplification of the reference gene *RpL32* was used as a control of total mRNA level. (**B**) Anti-LAMP2 immunostaining in adult brains reveals expression of the LAMP2A protein in *elav>LAMP2A* flies (panel ii) and not in *UAS-LAMP2A*/+ (*Lamp2*a/+) control (panel i). Note that a single optical section is shown at the level of the mushroom body lobes because the signal was too intense in panel ii to show a projection of the whole brain. Other sections show that expression was equally high in all parts of the brain, including in the optic lobes. Scale bars: 100 µm. (Related to Fig. 1).

**Figure S2.** LAMP2A prevents $SNCA^{A30P}$-associated increase in brain ROS level. (**A**) RT-PCR analysis performed on adult head RNA indicates no reduction in $SNCA^{A30P}$ or LAMP2A transcripts when both transgenes are coexpressed in neurons compared to expression of each transgene alone. *elav>LAMP2A*, $SNCA^{A30P}$ flies rather showed apparent increase in $SNCA^{A30P}$ mRNA levels compared to *elav*>$SNCA^{A30P}$ flies (left panel) and similar *LAMP2A* mRNA levels compared to *elav>LAMP2A* flies (right panel). Expression of both transgenes was absent in the driver alone flies *(elav/+)* and very low in the UAS construct alone flies ($SNCA^{A30P}$/+, *LAMP2A*/+ and *LAMP2A*, $SNCA^{A30P}$/+). Amplification of the reference gene *RpL32* was used as a control of total mRNA

level. (**B**) Representative scans of DHE-labelled brain from adult flies at 2 (top panels) and 30 (bottom panels) days a.E. showing differences in ROS levels. Fluorescence intensity was increased in brains of *elav>SNCA*$^{A30P}$ flies compared to *elav*/+ controls (*elav*), and it was brought back to control levels in brains of *elav>LAMP2A*, *SNCA*$^{A30P}$ flies. Scale bar: 100 µm. (Related to Fig. 2).

**Figure S3.** Lack of effect of LAMP2A on selective autophagy in the larval fat body. (**A**) In 3rd-instar larval fat body cells expressing KFERQ-Split-Venus eMI biosensor, reconstituted Split-Venus-positive fluorescent puncta were not detected under fed condition (panels i, ii) but were induced by 4 h of starvation (panels iii, iv), either in controls (*cg>KFERQ-Split-Venus-NC*, panels i, iii) or in larvae coexpressing LAMP2A (*cg>KFERQ-Split-Venus-NC, LAMP2A* flies, panels ii, iv). Examples of puncta are indicated by arrowheads. Note that the fluorescence gain has been set to a higher value for the pictures of panels iii and iv to allow for a clear display of the puncta. The cells that appear brightly fluorescent in these 2 panels actually had similar fluorescence levels as the cells in panels i and ii and did not show puncta. Scale bars: 30 µm. (**B, C**) Quantification of overall fluorescence intensity and puncta number per cell in fat body of larvae expressing KFERQ-Split-Venus eMI biosensor with or without (control) LAMP2A. Fluorescence intensity in fed or starvation conditions (**B**) and starvation-induced sensor puncta formation (**C**) were not increased by LAMP2A expression. (Related to Fig. 3A and B).

**Figure S4.** Representative fluorescent scans of whole-mount brains and mushroom body calyx region from adult *Drosophila* expressing KFERQ-Split-Venus sensor in all neurons. (**A**) Whole-

mount brains of flies expressing KFERQ-Split-Venus sensor without (*elav>KFERQ-Split-Venus-NC*, panels i and iii) or with (*elav>KFERQ-Split-Venus-NC, LAMP2A*, panels ii and iv) LAMP2A coexpression, under fed (panels i and ii) or starvation (panels iii and iv) conditions. Fluorescence was prominent in a posterior region comprising the calyx (ca) of the mushroom bodies (Mb). Kc, cell bodies of the mushroom body intrinsic Kenyon cells. Scale bars: 100 µm. (**B**) Representative pictures of the calyx region in brains revealing reconstituted KFERQ-Split-Venus-positive fluorescent puncta at high resolution (examples are indicated by arrowheads in panel i). The images are shown in negative to allow a better visualization of the puncta. Same panel nomenclature as in A. Results of puncta quantification are shown in Fig. 3E. Scale bars: 20 µM. (Related to Fig. 3D and E).

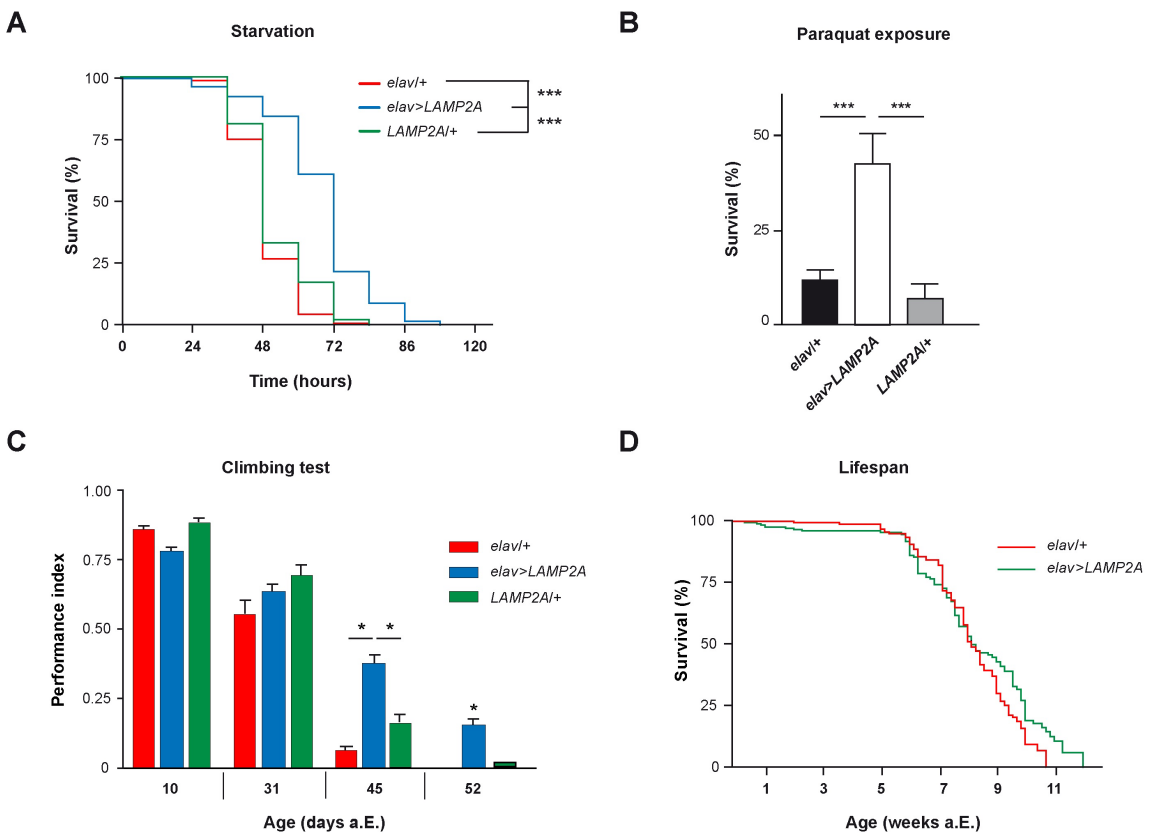


**Figure 1.** The LAMP2A receptor promotes stress resistance and neuroprotection in *Drosophila*. (**A**) Starvation resistance. Expression of the human LAMP2A protein in all neurons significantly extended *Drosophila* survival upon prolonged starvation (*elav>LAMP2A* flies) compared to *elav-Gal4*/+ (*elav*/+) driver and *UAS-LAMP2A*/+ (*LAMP2A*/+) effector controls. (**B**) Paraquat exposure. Survival of *elav>LAMP2A* flies fed with 20 mM paraquat for 72 h was markedly increased compared to the *elav*/+ and *LAMP2A*/+ controls. (**C**) Effect on age-related locomotor decline. Pan-neuronal LAMP2A expression (*elav>LAMP2A* flies) significantly delayed age-related decrements in climbing performance (SING assay) compared to driver and effector controls that behaved like the wild type. (**D**) Lifespan assay. *elav*/+ and *elav>LAMP2A* flies showed similar longevity curves (median lifespan 57 and 55 days, respectively) indicating that neuronal LAMP2A expression does not affect *Drosophila* lifespan.

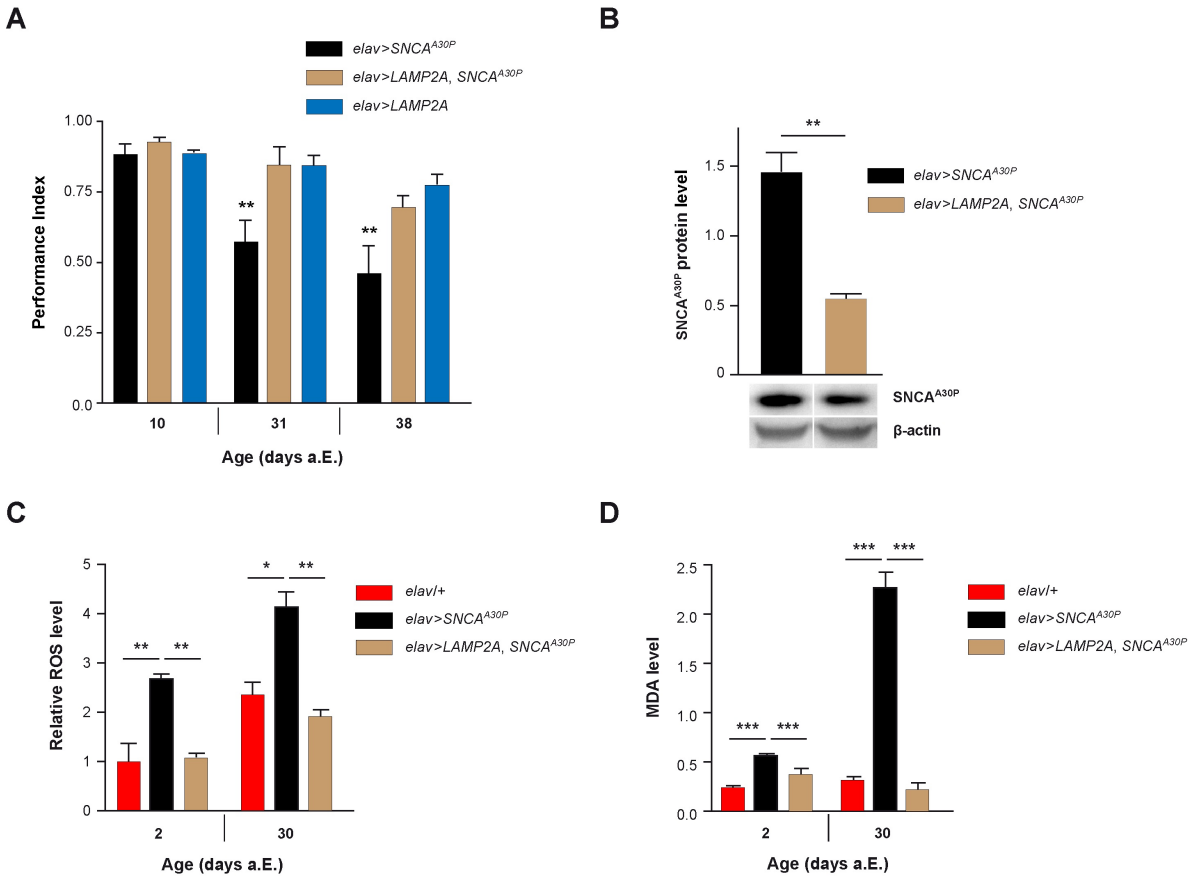


Issa et al. Figure 2

**Figure 2.** LAMP2A prevents SNCA-induced behavioral and oxidative defects in *Drosophila*. (**A**) LAMP2A coexpression fully prevented the progressive locomotor defects induced by pan-neuronal SNCA$^{A30P}$. Climbing ability (SING assay) of *elav>LAMP2A, SNCA$^{A30P}$* flies was compared to that of *elav>SNCA$^{A30P}$* and *elav>LAMP2A* flies at 10, 31 and 38 days after a.E. (**B**) Human LAMP2A reduced neuronal SNCA accumulation. Western blots of head protein extracts from 30-day-old *elav>SNCA$^{A30P}$* flies compared to *elav>LAMP2A, SNCA$^{A30P}$* probed with anti-SNCA antibody. Act5C was used as a loading control. Quantification of SNCA$^{A30P}$ protein level from 3 independent experiments. Coexpression of LAMP2A reduced SNCA$^{A30P}$ accumulation without decreasing its mRNA level (see Fig. S2A). (**C**) Brain ROS levels in the brain of *elav>LAMP2A, SNCA$^{A30P}$* flies were lower than those of *elav>SNCA$^{A30P}$*and comparable to the *elav*/+ control at both 2 and 30 days a.E. Representative pictures of DHE-labeled brain are shown in Fig. S2B. (**D**) MDA concentration assayed in the brain of 2- and 30-day-old adult *Drosophila* as an index of lipid peroxidation. Brain MDA level was markedly increased in *elav>SNCA$^{A30P}$* flies but not in *elav>LAMP2A, SNCA$^{A30P}$* flies that show similar levels as the *elav*/+ control.

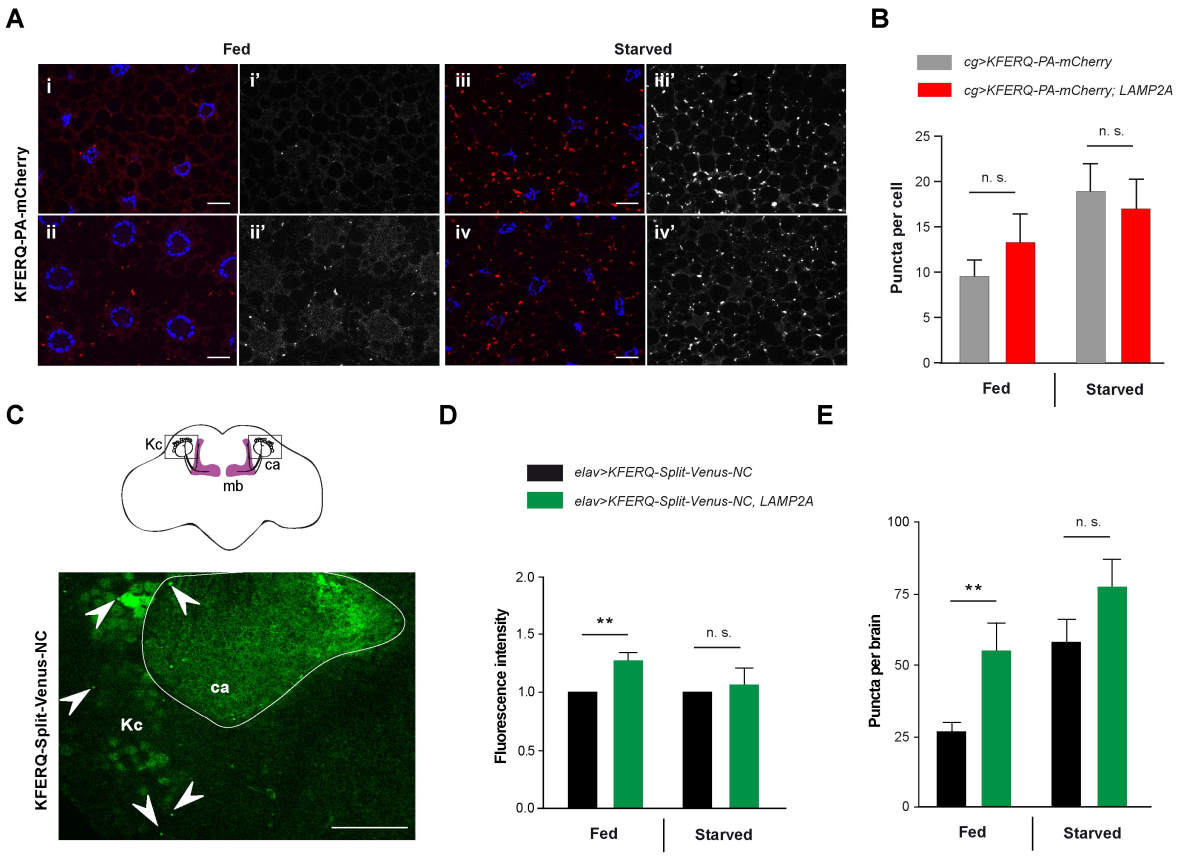


Issa et al. Figure 3

**Figure 3.** Effect of LAMP2A on selective autophagy in the larval fat body and adult brain. (**A**) In 3rd-instar larval fat body cells, LAMP2A expression (*LAMP2A*, bottom panels) did not increase KFERQ-PA-mCherry fluorescent sensor puncta formation 25 h after photoactivation, either under fed (i, ii) or starvation (iii, iv) conditions, compared to controls (top panels). In composite images, mCherry fluorescence is in red and DAPI-stained nuclei are in blue. i'-iv' monochromatic images show the KFERQ-PA-mCherry single channel. Scale bars: 20 µm. (**B**) Quantification of puncta number per cell in larvae expressing photoactivated KFERQ-PA-mCherry in fat body with or without (control) LAMP2A under fed or starvation conditions. Starvation-induced sensor puncta formation was not further increased by LAMP2A expression. Similar results were obtained using a different eMI biosensor (KFERQ-Split-Venus) (shown in Fig. S3). (**C**) Localization of reconstituted KFERQ-Split-Venus sensor fluorescent puncta (arrowheads) in a posterior region of the adult brain of *elav>KFERQ-Split-Venus-NC* flies expressing the eMI sensor in all neurons. The square in the scheme (top inset) shows localization of the magnified brain region that surrounds the calyx of the mushroom body, where fluorescence was prominent and in which puncta were scored. Mb, mushroom body; Kc, cell bodies of the Mb Kenyon cells; ca,

calyx. Representative scans of whole brain and calyx region for the different genotypes and feeding conditions are shown in Fig. S4A and B, respectively. (**D, E**) Reconstitution of KFERQ-Split-Venus eMI sensor was increased in adult brain of fed, but not starved, flies expressing LAMP2A in all neurons (*elav>KFERQ-Split-Venus-NC*, *LAMP2A*) (*LAMP2A*, right panel), as indicated by higher overall fluorescence level (**D**) and increased density of eMI-positive puncta in the calyx region (**E**), compared to *elav>KFERQ-Split-Venus-NC* controls. Quantification from 3 independent experiments.

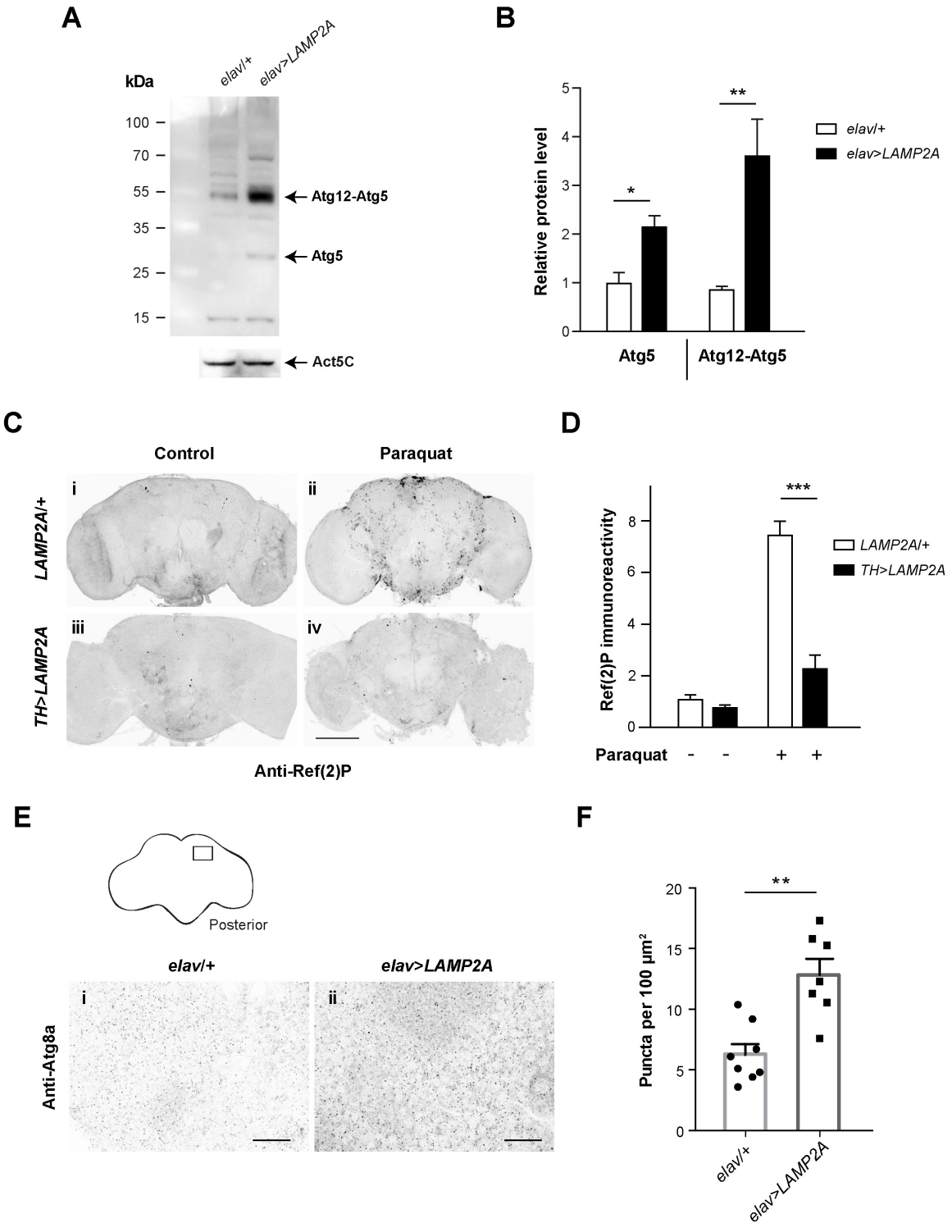


Issa et al. Figure 4

**Figure 4.** Human LAMP2A enhances macroautophagy in the *Drosophila* brain. (**A, B**) Effect of LAMP2A on Atg5 expression. (**A**) Western blot of head protein extracts from 10-day old control flies (*elav*/+) and flies expressing human LAMP2A in neurons (*elav>LAMP2A*) probed with anti-Atg5 antibody. LAMP2A expression markedly increased levels of Atg5 and of the Atg12-Atg5 complex that is required for autophagosome formation. Act5C served as a loading control. (**B**) Quantification of Atg5 protein and the Atg12-Atg5 complex from 3 independent western blot experiments. (**C, D**) Effect of LAMP2A on paraquat-induced Ref(2)P accumulation. (**C**) Anti-Ref(2)P immunostaining in whole-mount adult brains of *LAMP2A*/+ (panels i and ii) and *TH>LAMP2A* (panels iii and iv) flies exposed to paraquat (panels ii and iv) or not (panels i and iii). LAMP2A expression prevented paraquat-induced Ref(2)P accumulation (black puncta) suggesting that the human protein is able to maintain efficient autophagic flux under oxidative stress. Scale bar: 100 µm. (**D**) Quantification of Ref(2)P immunostaining in the central brain region normalized to *LAMP2A*/+ control not exposed to paraquat (n = 4 or 5 independent brains per condition). (**E, F**) Effect of LAMP2A on the number of Atg8a-positive puncta. (**E**) Anti-Atg8a immunostaining in whole-mount adult brains of *elav*/+ (panel i) and *elav>LAMP2A* (panel ii) flies. The inset scheme on top shows the posterior neuropil region that was magnified in panels i and ii and in which Atg8a puncta were counted. Scale bars: 10 µm. (**F**) Quantification of Atg8a-positive dots. Each black circle (*elav*/+) or square (*elav>LAMP2A*) represents the score for a different brain. The number of Atg8a puncta that reflect autophagosome formation was markedly increased in LAMP2A-expressing flies. Similar results were obtained in 3 independent experiments.

# The lysosomal membrane protein LAMP2A promotes autophagic flux and prevents SNCA-induced Parkinson disease-like symptoms in the *Drosophila* brain

Abdul-Raouf Issa, Jun Sun, Céline Petitgas, Ana Mesquita, Amina Dulac, Marion Robin, Bertrand Mollereau, Andreas Jenny, Baya Chérif-Zahar, and Serge Birman

## SUPPLEMENTARY INFORMATION

**Tables S1-S3**

**Figures S1-S4**

**Table S1.** Primers used for human *LAMP2A* cDNA cloning.

| Gene* | GeneBank Accession | Primers | Sequences* |
|---|---|---|---|
| *LAMP2A* | X77196.1 | P1-*Bgl*II (forward)** | 5’-gccgcc**agatct**gctacaaaatggtgtgcttccgcctctt |
| | | P2-*Xho*I (reverse) | 5’-atcaat**ctcgag**gcagattctaaaattgctcat |

*The added restriction sites are in bold type.

**The bases modified to match the *Drosophila* translation start consensus sequence are underlined.

**Table S2.** Primers used for RT-PCR and real-time PCR.

| Gene* | GeneBank Accession | Primers | Sequences |
|---|---|---|---|
| *LAMP2A* | X77196.1 | *LAMP2A* (forward) | 5’-gatctgctacaaaatggtgtgcttccg |
| | | *LAMP2A* (reverse) | 5’-atcaatctcgaggcagattctaaaattgctcat |
| *SNCA* | L08850.1 | *SNCA* (forward) | 5'-ctccaaaaccaaggagggagt |
| | | *SNCA* (reverse) | 5'-gcctcattgtcaggatccaca |
| *RpL32* | NM_079843.4 | *RpL32* (forward) | 5'-gacgcttcaagggacagtatc |
| | | *RpL32* (reverse) | 5'-aaacgcggttctgcatgag |

**Table S3.** Statistical data of the starvation experiments (related fo Fig. 1A).

| Genotype | Fly number per trial | Number of trial | Median lifespan (hours) | Maximum lifespan (hours) | Log-rank test Chi² | Log-rank test P-value |
|---|---|---|---|---|---|---|
| *elav* | 50 | 3 | 48 | 84 | 6.391 | 0.0115 |
| *LAMP2A* | 50 | 3 | 48 | 84 | | |
| *elav* | 50 | 3 | 48 | 84 | 111.3 | <0,0001 |
| *elav>LAMP2A* | 50 | 3 | 72 | 108 | | |
| *LAMP2A* | 50 | 3 | 48 | 84 | 68.70 | <0,0001 |
| *elav>LAMP2A* | 50 | 3 | 72 | 108 | | |

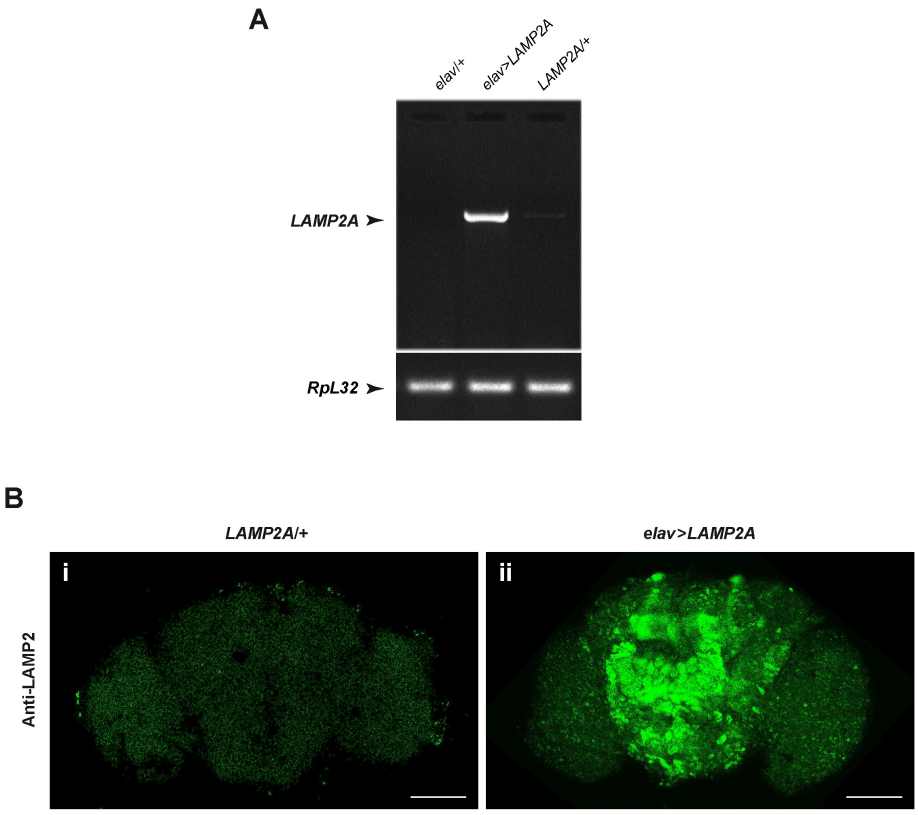


**Figure S1.** Expression of human LAMP2A in transgenic flies. (**A**) RT-PCR analysis performed on adult head RNAs detects *LAMP2A* mRNA in *elav>LAMP2A* flies and not in *elav-Gal4*/+ (*elav*/+) control. The tiny band amplified in the *UAS-LAMP2A/+* (*LAMP2A*/+) control could originate from a small amount of Gal4-independent transgene expression or genomic DNA contamination. Amplification of the reference gene *RpL32* was used as a control of total mRNA level. (**B**) Anti-LAMP2 immunostaining in adult brains reveals expression of the LAMP2A protein in *elav>LAMP2A* flies (panel ii) and not in *UAS-LAMP2A*/+ (*Lamp2*a/+) control (panel i). Note that a single optical section is shown at the level of the mushroom body lobes because the signal was too intense in panel ii to show a projection of the whole brain. Other sections show that expression was equally high in all parts of the brain, including in the optic lobes. Scale bars: 100 µm. (Related to Fig. 1).

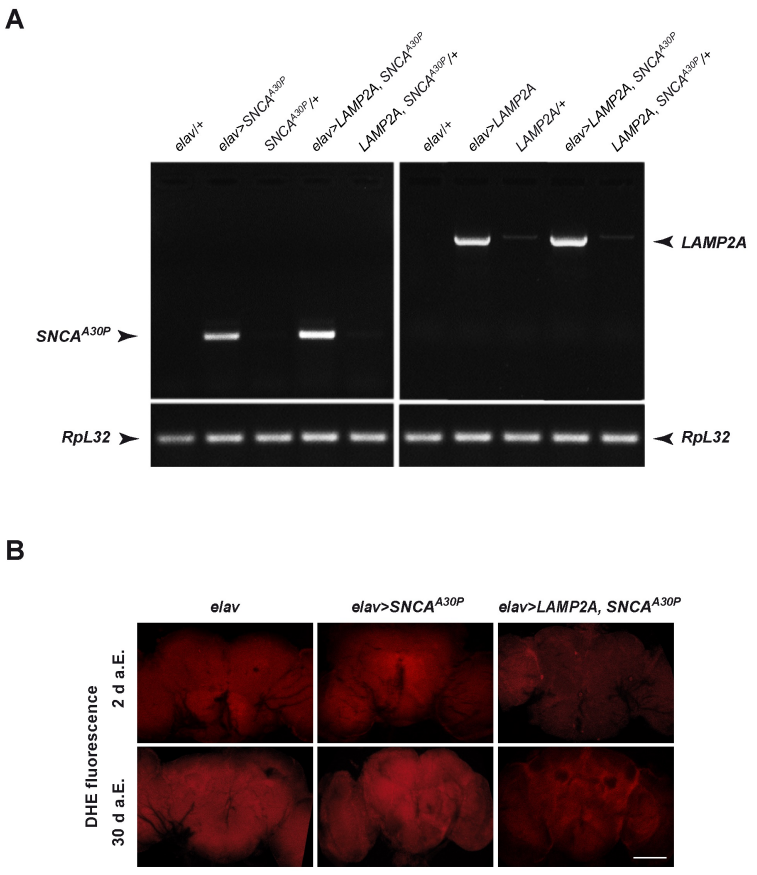


Issa et al. Figure S2

**Figure S2.** LAMP2A prevents SNCA$^{A30P}$-associated increase in brain ROS level. (**A**) RT-PCR analysis performed on adult head RNA indicates no reduction in SNCA$^{A30P}$ or LAMP2A transcripts when both transgenes are coexpressed in neurons compared to expression of each transgene alone. *elav>LAMP2A,* SNCA$^{A30P}$ flies rather showed apparent increase in SNCA$^{A30P}$ mRNA levels compared to *elav*>SNCA$^{A30P}$ flies (left panel) and similar *LAMP2A* mRNA levels compared to *elav>LAMP2A* flies (right panel). Expression of both transgenes was absent in the driver alone flies *(elav/+)* and very low in the UAS construct alone flies (SNCA$^{A30P}$/+, *LAMP2A*/+ and *LAMP2A*, SNCA$^{A30P}$/+). Amplification of the reference gene *RpL32* was used as a control of total mRNA level. (**B**) Representative scans of DHE-labelled brain from adult flies at 2 (top panels) and 30 (bottom panels) days a.E. showing differences in ROS levels. Fluorescence intensity was increased in brains of *elav>SNCA$^{A30P}$* flies compared to *elav*/+ controls (*elav*), and it was brought back to control levels in brains of *elav>LAMP2A*, *SNCA$^{A30P}$* flies. Scale bar: 100 µm. (Related to Fig. 2).

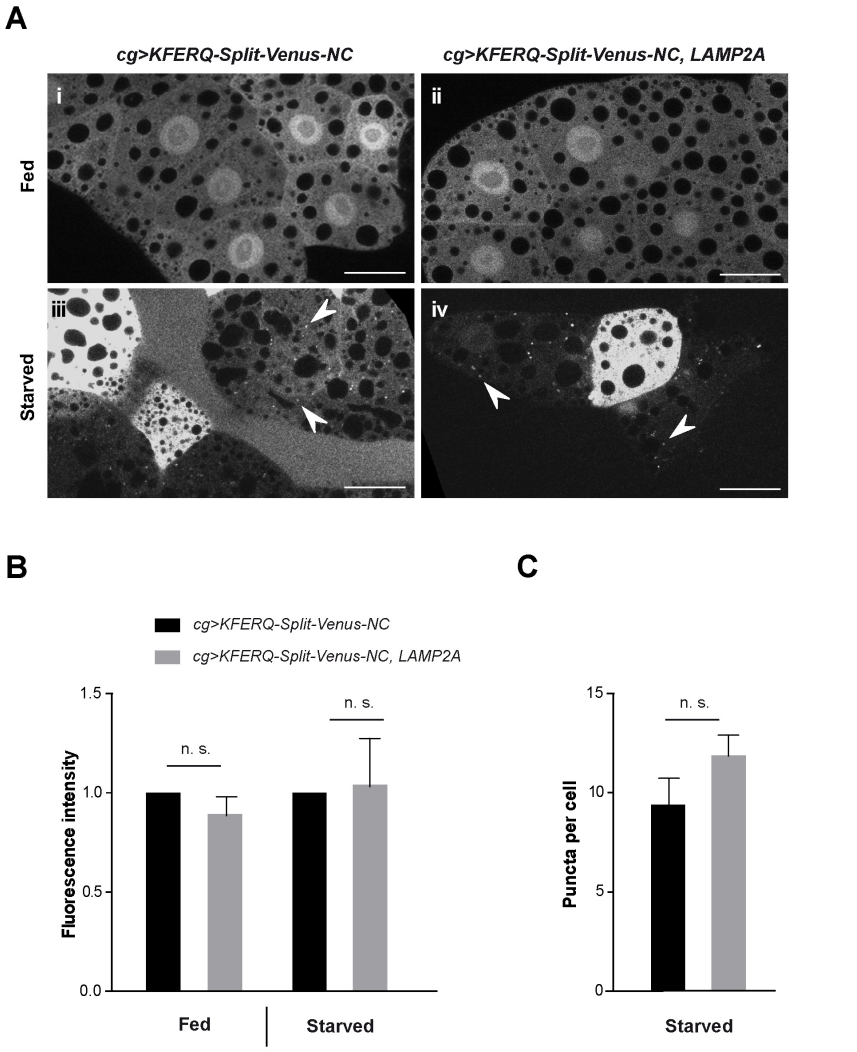


**Figure S3.** Lack of effect of LAMP2A on selective autophagy in the larval fat body. (**A**) In 3rd-instar larval fat body cells expressing KFERQ-Split-Venus eMI biosensor, reconstituted Split-Venus-positive fluorescent puncta were not detected under fed condition (panels i, ii) but were induced by 4 h of starvation (panels iii, iv), either in controls (*cg>KFERQ-Split-Venus-NC*, panels i, iii) or in larvae coexpressing LAMP2A (*cg>KFERQ-Split-Venus-NC, LAMP2A* flies, panels ii, iv). Examples of puncta are indicated by arrowheads. Note that the fluorescence gain has been set to a higher value for the pictures of panels iii and iv to allow for a clear display of the puncta. The cells that appear brightly fluorescent in these 2 panels actually had similar fluorescence levels as the cells in panels i and ii and did not show puncta. Scale bars: 30 µm. (**B, C**)

Quantification of overall fluorescence intensity and puncta number per cell in fat body of larvae expressing KFERQ-Split-Venus eMI biosensor with or without (control) LAMP2A. Fluorescence intensity in fed or starvation conditions (**B**) and starvation-induced sensor puncta formation (**C**) were not increased by LAMP2A expression. (Related to Fig. 3A and B).

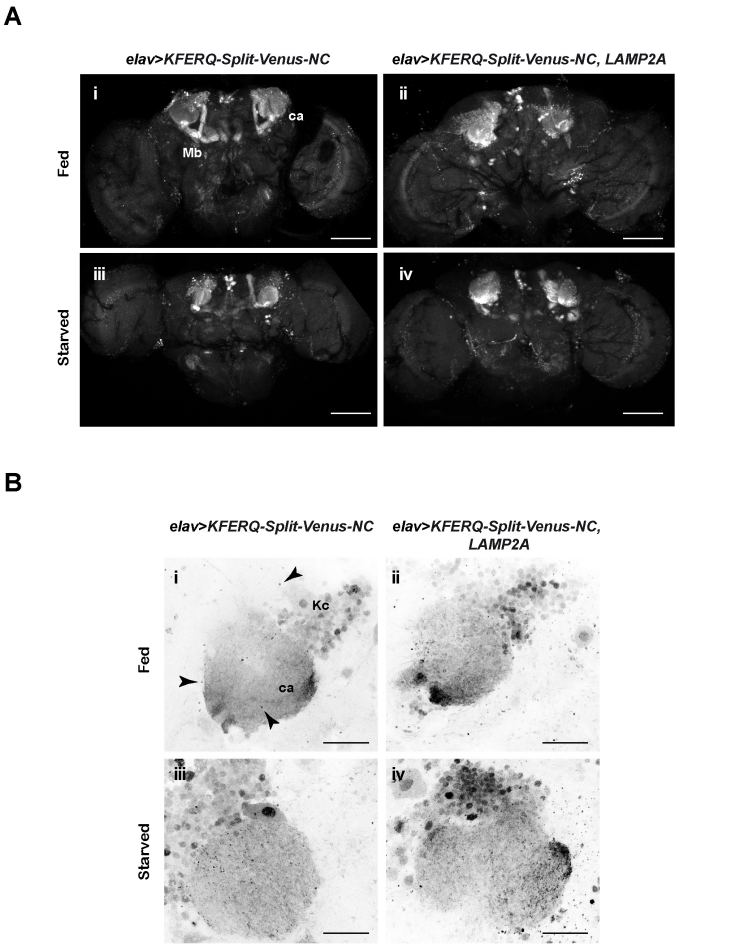


**Figure S4.** Representative fluorescent scans of whole-mount brains and mushroom body calyx region from adult *Drosophila* expressing KFERQ-Split-Venus sensor in all neurons. (**A**) Whole-mount brains of flies expressing KFERQ-Split-Venus sensor without (*elav>KFERQ-Split-Venus-NC*, panels i and iii) or with (*elav>KFERQ-Split-Venus-NC, LAMP2A*, panels ii and iv) LAMP2A coexpression, under fed (panels i and ii) or starvation (panels iii and iv) conditions. Fluorescence was prominent in a posterior region comprising the calyx (ca) of the mushroom bodies (Mb). Kc, cell bodies of the mushroom body intrinsic Kenyon cells. Scale bars: 100 µm. (**B**) Representative pictures of the calyx region in brains revealing reconstituted KFERQ-Split-Venus-positive fluorescent puncta at high resolution (examples are indicated by arrowheads in panel i). The images are shown in negative to allow a better visualization of the puncta. Same panel nomenclature as in A. Results of puncta quantification are shown in Fig. 3E. Scale bars: 20 µM. (Related to Fig. 3D and E).